


RESEARCH ARTICLE OPEN ACCESS

Genetic Dissection of Cyclic di-GMP Signalling in *Pseudomonas aeruginosa* via Systematic Diguanylate Cyclase Disruption

Román A. Martino^{1,2} | Daniel C. Volke³ | Albano H. Tenaglia^{1,2} | Paula M. Tribelli^{4,5} | Pablo I. Nikel³  | Andrea M. Smania^{1,2}

¹Universidad Nacional de Córdoba, Facultad de Ciencias Químicas, Departamento de Química Biológica Ranwel Caputto, Córdoba, Argentina | ²CONICET, Universidad Nacional de Córdoba, Centro de Investigaciones en Química Biológica de Córdoba (CIQUIBIC), Córdoba, Argentina | ³The Novo Nordisk Foundation Center for Biosustainability, Technical University of Denmark, Kongens Lyngby, Denmark | ⁴Universidad de Buenos Aires, Facultad de Ciencias Exactas y Naturales, Departamento de Química Biológica, Buenos Aires, Argentina | ⁵CONICET, Universidad de Buenos Aires, Instituto de Química Biológica de la Facultad de Ciencias Exactas y Naturales (IQUIBICEN), Buenos Aires, Argentina

Correspondence: Pablo I. Nikel (pabnik@biosustain.dtu.dk) | Andrea M. Smania (asmania@unc.edu.ar)

Received: 27 January 2025 | **Revised:** 8 March 2025 | **Accepted:** 10 March 2025

Funding: This work was supported by Agencia Nacional de Promoción Científica y Tecnológica (PICT-2019-1590); HORIZON EUROPE Climate, Energy and Mobility (101082049); Secretaría de Ciencia y Tecnología de la Universidad Nacional de Córdoba (33620180100413CB); Consejo Nacional de Investigaciones Científicas y Técnicas (PIP-2022-11220210100945CO); H2020 LEIT Biotechnology (814418); Novo Nordisk Fonden (NNF18OC0034818, NNF20CC0035580, NNF21OC0067996, NNF23OC0083631, NNF24OC0091501); Research and Training Grant from the Federation of European Microbiological Societies (FEMS).

Keywords: biofilms | c-di-GMP | CRISPR/Cas9 | Diguanylate cyclases | microbial physiology | *Pseudomonas aeruginosa* | synthetic biology

ABSTRACT

The second messenger *bis*-(3' → 5')-cyclic dimeric guanosine monophosphate (c-di-GMP) governs adaptive responses in the opportunistic pathogen *Pseudomonas aeruginosa*, including biofilm formation and the transition from acute to chronic infections. Understanding the intricate c-di-GMP signalling network remains challenging due to the overlapping activities of numerous diguanylate cyclases (DGCs). In this study, we employed a CRISPR-based multiplex genome-editing tool to disrupt all 32 GGDEF domain-containing proteins (GCPs) implicated in c-di-GMP signalling in *P. aeruginosa* PA14. Phenotypic and physiological analyses revealed that the resulting mutant was unable to form biofilms and had attenuated virulence. Residual c-di-GMP levels were still detected despite the extensive GCP disruption, underscoring the robustness of this regulatory network. Taken together, these findings provide insights into the complex c-di-GMP metabolism and showcase the importance of functional overlapping in bacterial signalling. Moreover, our approach overcomes the native redundancy in c-di-GMP synthesis, providing a framework to dissect individual DGC functions and paving the way for targeted strategies to address bacterial adaptation and pathogenesis.

1 | Introduction

Bacterial survival depends on the precise coordination of extracellular and intracellular signals to adapt to environmental changes (Wu et al. 2011). These signals are conveyed through

diverse small molecules that interact with complex regulatory networks, ultimately controlling bacterial growth and behaviour. Cyclic dinucleotides, especially *bis*-(3' → 5')-cyclic dimeric guanosine monophosphate (cyclic di-GMP, henceforth referred to as c-di-GMP), are versatile second messengers

Román A. Martino and Daniel C. Volke contributed equally to this work.

This is an open access article under the terms of the [Creative Commons Attribution-NonCommercial-NoDerivs](https://creativecommons.org/licenses/by-nc-nd/4.0/) License, which permits use and distribution in any medium, provided the original work is properly cited, the use is non-commercial and no modifications or adaptations are made.

© 2025 The Author(s). *Microbial Biotechnology* published by John Wiley & Sons Ltd.

(Junkermeier and Hengge 2023), regulating numerous physiological processes in bacteria (Jenal et al. 2017). c-di-GMP, one of the earliest discovered and most widespread second messengers in bacteria, is synthesised by diguanylate cyclases (DGCs) with GGDEF domains and degraded by phosphodiesterases (PDEs) containing EAL or HD-GYP domains. However, not all GGDEF-containing proteins (GCPs) are active DGCs; some lack enzymatic activity and instead regulate c-di-GMP signalling pathways (Hengge 2021). Similarly, certain EAL- or HD-GYP-containing proteins do not function as PDEs but fulfil other roles (Galperin and Chou 2022). DGCs and PDEs respond to internal and external stimuli, adjusting c-di-GMP levels and initiating specific regulatory responses through interactions with effector molecules (Hengge 2009; Römling et al. 2013; Ryan 2013).

A key cellular process regulated by c-di-GMP is the reversible switch between motile and sessile states as bacteria transition from planktonic forms to biofilms (Oladosu et al. 2024). Biofilms are surface-attached bacterial communities embedded in a self-produced matrix (Costerton 2001; Mah and O'Toole 2001; Gjermansen et al. 2005; Luján et al. 2011; La Rosa et al. 2018). Beyond controlling the motile-sessile transition, c-di-GMP influences essential bacterial processes, including virulence, morphogenesis, and stress responses (Dahlstrom and O'Toole 2017). Given the central role of c-di-GMP, DGCs and PDEs are the subjects of intense research and constitute promising targets for the design of novel drugs to combat antimicrobial resistance (Winstanley et al. 2016).

Bacterial species display a variable number of c-di-GMP-metabolising enzymes. Obligate pathogens often have fewer of these enzymes compared to free-living species (Bobrov et al. 2011; Dahlstrom and O'Toole 2017). The apparent redundancy of such proteins in free-living bacteria supports the regulatory flexibility needed to adapt to fluctuating environments. The opportunistic pathogen *Pseudomonas aeruginosa*, for instance, encodes up to 40 GGDEF-, EAL-, or HD-GYP-domain proteins, or dual-domain variants, many of which are known to be involved in c-di-GMP metabolism (Kulasakara et al. 2006). *P. aeruginosa* causes severe infections in individuals with compromised defences, burns, or cystic fibrosis, often leading to high morbidity and mortality (Rosenthal et al. 2016; Brinkman et al. 2021). Treating *P. aeruginosa* infections is especially challenging due to a wide array of virulence factors and a remarkable capacity to resist antibiotics (Colque et al. 2022; Cordisco and Serra 2025; Macesic et al. 2025; Molinari et al. 2025; Timmis et al. 2025). Furthermore, *P. aeruginosa* forms robust biofilms that evade immune clearance and impair antibiotic efficacy. The complexity of the c-di-GMP signalling network, which regulates exopolysaccharide production, biofilm formation, motility, virulence, and antibiotic resistance, underlies the adaptability and pathogenicity of this species (Hengge 2009; Valentini and Filloux 2016; Jenal et al. 2017).

Several approaches have been used to explore the role of c-di-GMP metabolising enzymes in *P. aeruginosa*, including targeted deletions to create single mutants through specific or random (transposon) mutagenesis (Kulasakara et al. 2006; Ha et al. 2014; Nie et al. 2020; Eilers et al. 2022). However, these methods failed to address redundancy or compensatory effects among different enzymes. For example, single deletions of these proteins often produce no detectable phenotypic changes. Complementary

strategies that examine individual DGCs in the absence of other c-di-GMP-synthesising and processing enzymes would provide valuable insights into their specific roles and interactions by establishing interference-free systems. This purpose has been fulfilled by mutating genes that encode c-di-GMP-synthesising proteins in *Salmonella enterica* (Solano et al. 2009), *Caulobacter crescentus* (Abel et al. 2013), *Sinorhizobium (Ensifer) meliloti* (Schäper et al. 2016), and *Dickeya zeae* (Chen et al. 2020), through the removal of 12, 11, 15, and 16 GCPs, respectively. However, depleting all GCPs in the complex *P. aeruginosa* c-di-GMP signalling network remains a significant challenge, requiring extensive genome engineering that traditional methods cannot achieve efficiently. CRISPR-associated technologies offer new possibilities in bacterial genome engineering (Volke, Gurdo et al. 2023; Volke, Orsi et al. 2023; Kozaeva et al. 2024; Krink et al. 2024), enabling multiple genetic modifications in a cost- and time-efficient manner.

In this study, we applied a CRISPR/Cas9-based multiplex genome-editing tool to target all 32 GCP-encoding genes in *P. aeruginosa* UCBPP-PA14 (henceforth referred to as *P. aeruginosa* PA14). We then examined how the absence of these proteins affected multiple physiological and metabolic traits, including cell growth, biofilm formation, virulence factor expression, competitiveness, antibiotic resistance, and motility. Genetic complementation with selected DGCs in the resulting mutant, termed *P. aeruginosa* PA14 Δ 32, revealed diverse effects on c-di-GMP-related traits. These results shed new light on the multifaceted role of GCPs under conditions where all such proteins are disrupted, overcoming pathway redundancy and emphasising the complexity and adaptability of c-di-GMP metabolism in this model opportunistic pathogen.

2 | Experimental Procedures

2.1 | Molecular Biology Techniques and Construction of *P. aeruginosa* PA14 Δ 32

The bacterial strains and oligonucleotide sequences used in this study are listed in Tables S1 and S2 in the Supporting Information, respectively. All kits and enzymes were used according to the manufacturer's recommendations. Plasmid and DNA purifications were performed using the NucleoSpin Plasmid EasyPure mini kit and NucleoSpin Gel and PCR clean-up mini kit (Macherey-Nagel, Düren, Germany). PCR amplifications employed Phusion U high-fidelity DNA polymerases (Thermo Fisher Scientific, Waltham, MA, USA) and OneTaq Quick-Load 2 \times master mix (New England Biolabs, Ipswich, MA, USA). All restriction enzymes were FastDigest (Thermo Fisher Scientific), while the USER enzyme (New England Biolabs) was used for USER-cloning procedures. Sanger sequencing was carried out using the Mix2Seq kit (Eurofins Genomics GmbH, Ebersberg, Germany).

The locus tags of the GGDEF domain-containing proteins were obtained from previous studies (Kulasakara et al. 2006; Ha et al. 2014) and verified using the *Functional Domain Annotations* tool available at the [Pseudomonas.com](https://pseudomonas.com) database (Winsor et al. 2016) through a bioinformatic search for all annotated nucleotide cyclase enzymes. The construction of the pBEC/pMBEC plasmid for base editing and genetic modifications of *P. aeruginosa* followed the methodology of Volke et al. (2022). Spacer sequences

(20-nt, Table S1) were designed using the CRISPy web service (Blin et al. 2016) based on the GenBank sequence (NC_008463.1) of *P. aeruginosa* PA14 (Rahme et al. 1995; Liberati et al. 2006; Ozer et al. 2014; Winsor et al. 2016). Spacers used in the study are listed in Table S2. The synthetic spacers were cloned into pBEC/pMBEC vectors via Golden Gate assembly (Bird et al. 2022), and each construct was verified through Sanger sequencing. For genome editing, *P. aeruginosa* PA14 was electroporated with pBEC/pMBEC plasmids containing different spacer combinations targeting genes encoding diguanylate cyclases. Cells were incubated in lysogeny broth (LB) for 3 h to recover, followed by inoculation of 100 μ L into 10 mL of LB with 30 μ g mL⁻¹ gentamicin and incubation overnight (ON, ca. 16 h) at 37°C with agitation at 200 rpm. To cure the base editing plasmid, 100 μ L of the culture was transferred to 10 mL of LB containing 10% (w/v) sucrose and incubated ON. Dilutions of the culture were plated on LB agar to isolate individual colonies. For each base editing event, the genomes of 5–10 randomly selected colonies were sequenced to confirm the introduction of premature *STOP* codons in the target genes.

2.2 | Bacterial Strains, Plasmids, and Culture Conditions

Escherichia coli and *P. aeruginosa* were routinely incubated at 37°C in LB. Routine cloning was performed in laboratory *E. coli* strains according to standard protocols (Volke, Friis et al. 2020; Wirth et al. 2020; Wirth, Funk et al. 2023; Wirth, Rohr et al. 2023; Kozaeva et al. 2021). Whenever necessary, antibiotics were used at the following concentrations: 10 μ g mL⁻¹ gentamicin, 100 μ g mL⁻¹ ampicillin, 50 μ g mL⁻¹ kanamycin, 30 μ g mL⁻¹ chloramphenicol, and 50 μ g mL⁻¹ streptomycin for *E. coli*; and 30 μ g mL⁻¹ gentamicin, 25 μ g mL⁻¹ tetracycline, and 250 μ g mL⁻¹ streptomycin for *P. aeruginosa*. Bacterial growth was monitored by measuring the optical density at 600 nm (OD₆₀₀); growth parameters were calculated as described by Wirth, Funk et al. (2023).

2.3 | Whole-Genome Sequencing and Identification of Off-Target Mutations

Whole-genome sequencing was conducted using an Illumina Novaseq 6000 platform (Novogene Co., San Jose, CA, USA). Reads were mapped against the *P. aeruginosa* PA14 reference genome using the Geneious platform (Dotmatics, Boston, MA, USA). Sequences were trimmed and normalised before alignment. Single nucleotide polymorphisms (SNPs) and small insertions or deletions (indels) were identified via variant calling with a variant frequency threshold of 0.4 for all samples. A lower threshold of 0.1 was applied to the negative control to detect pre-existing nucleotide polymorphisms in the parental strain (Fernández-Cabezón et al. 2021).

2.4 | Phenotypic Characterisation

2.4.1 | Colony Morphology

Strains were cultivated ON at 37°C with agitation in LB. Subsequently, cultures were diluted and plated on LB agar to yield 30–50 colonies per plate, followed by incubation for 16 h

at 37°C. Antibiotics or inducers were added to LB and LB agar plates as required for the specific assay. Colony morphology pictures were then taken as described elsewhere (Volke, Turlin et al. 2020).

2.4.2 | Motility Assays

Swarming motility assays were conducted on M8 plates (Köhler et al. 2001) containing 0.5% (w/v) agar and incubated for 48 h at 37°C, following the protocol by Caiazza et al. (2005). Swimming motility assays were performed in tryptone plates with 0.3% (w/v) agar, incubated for 24 h at 37°C. Twitching motility assays were carried out in LB agar plates containing 1% (w/v) agar, incubated for 24 h at 37°C and then for 48 h at room temperature, as described by Smania et al. (2004).

2.4.3 | Biofilm Formation

Biofilm formation was quantified using the crystal violet staining (CVS) method in a 96-well microtiter plate (Navarro et al. 2011). Replicates of the different strains were incubated overnight, and cultures were adjusted to a cell density of 1.5×10^6 colony forming units (CFU) mL⁻¹. A 100- μ L aliquot of each culture was seeded in triplicate into a 96-well microtiter plate and incubated at 37°C for 16 h. After incubation, biofilms were stained with crystal violet, and the absorbance was measured at 595 nm in an Epoch Microplate Spectrophotometer (BioTek Instruments Inc., Winooski, VT, USA).

Biofilm imaging of *P. aeruginosa* was performed as described by Moyano et al. (2020). Bacterial strains were grown in 8-well Lab-Tek chamber coverglass systems (Nunc, Thermo Fisher Scientific). Chambers were inoculated with 5×10^5 cells in 250 μ L of fresh medium and incubated for 24 h at 37°C. Biofilms were stained using the LIVE/DEAD BacLight bacterial viability kit (Molecular Probes Inc., Eugene, OR, USA), applying the SYTO 9 green-fluorescent nucleic acid stain according to the manufacturer's protocol. Images were captured with an FV1200 confocal microscope (Olympus, Tokyo, Japan) using a 60 \times oil super-corrected UPLXAPO60XO objective lens. Cell detection was performed with the default configuration of FV10 software (ASW 4.0; Evident, Waltham, MA, USA) for green emission fluorophores (SYTOX green nucleic acid stain; Sigma-Aldrich Co., St. Louis, MO, USA).

2.4.4 | Determination of Virulence-Associated Traits

Rhamnolipid production was assessed by observing red blood cell lysis on sheep blood agar plates (Britania S.A., Buenos Aires, Argentina). Plates were inoculated with 5 μ L of bacterial culture and incubated at 37°C for 96 h. Extracellular protease activity was evaluated using milk agar plates containing 1% (w/v) agar. Bacteria were first grown aerobically in tryptic soy broth at 37°C, after which 5 μ L of culture was spotted on milk agar plates and incubated ON at 37°C. Degradation halos and colony diameters were measured and quantified using ImageJ software (Fiji; Schindelin et al. 2012). Pyoverdine production was assessed in King's B medium (Smania et al. 2004) after cultures

were incubated at 37°C for 24 h with agitation at 220 rpm. A 1-mL aliquot of the culture was centrifuged at 10,000×g for 10 min, and the absorbance of the supernatant was measured at 360 nm. Pyocyanin production was measured in LB. Cultures were grown for 48 h at 220 rpm, followed by centrifugation of 2 mL at 10,000×g for 10 min. Pyocyanin was extracted from the supernatant with chloroform/HCl, and the absorbance of the extract was measured at 595 nm.

2.4.5 | Nematode Paralysis Assay

Nematode paralysis assays were conducted following the method by Luján et al. (2007). In brief, 10 mL aliquots of 1/10 dilutions of ON brain heart infusion (BHI) cultures were spread onto 5.5-cm diameter plates containing 10 mL of BHI with 1.2% (w/v) agar. Plates were incubated for 24 h at 30°C. *Caenorhabditis elegans* var. Bristol strain N2 nematodes were collected from stock plates using M9 buffer (containing 20 mM KH₂PO₄, 40 mM Na₂HPO₄, 90 mM NaCl, and 1 mM MgSO₄), and a 50-μL aliquot containing ca. 20–40 adult worms was spotted onto the *P. aeruginosa* lawn. Plates were incubated for 6 h at room temperature with lids on, after which the number of live nematodes was recorded. Worms were deemed paralysed if they failed to move spontaneously and showed no response to mechanical stimulation. *E. coli* strain OP50 (Xiao et al. 2015) was included as a non-virulent control, with each assay performed at least in triplicate.

2.4.6 | Transmission electron Microscopy

For transmission electron microscopy (TEM), strains were grown ON at 37°C on LB agar plates. Cells were then suspended in 1× PBS (containing 137 mM NaCl, 2.7 mM KCl, 10 mM Na₂HPO₄, and 1.8 mM KH₂PO₄, pH=7.4) by scraping the biomass from the agar plate surface. TEM imaging was carried out at the Transmission Electron Microscopy Services of Instituto de Investigaciones en Ciencias de la Salud (INICSA)-CONICET, Centro de Microscopía Electrónica (Facultad de Ciencias Médicas, Universidad Nacional de Córdoba, Córdoba, Argentina). Formvar-coated nickel grids were floated on a mixture of bacteria suspension and a 2% (v/v) H₃PW₁₂O₄₀ solution in a 1:1 ratio for 1 min. The grids were then rinsed briefly with distilled water, and excess liquid was removed using the edge of a filter paper disk. After air drying for 5 min, the specimens were examined in a Zeiss LEO906 TEM (Carl Zeiss AG, Oberkochen, Germany) operated at an accelerating voltage of 80 kV and photographed with a Megaview G3 camera (EMSIS GmbH, Münster, Germany).

2.4.7 | Expression of DGC Genes for Complementation Assays

Plasmids pJN_wspR and pJN_23130 (Table S1), carrying wild-type copies of PA14_16500 or PA14_23130 cloned in the pJN105 vector (Newman and Fuqua 1999), were used for the expression of DGC-encoding genes in complementation assays. In these constructs, the expression of PA14_16500 and PA14_23130 is driven by an arabinose-inducible expression system (Martínez-García et al. 2023; Wirth, Funk et al. (2023). For routine

complementation assays, transformed cells were cultured in LB or on LB agar plates supplemented with 0.1%–1% (w/v) arabinose. Additionally, a wild-type copy of *fimX* (PA14_65540) was cloned into the pMBLe vector, generating plasmid pMBLe_*fimX* (Colque et al. 2022), where *fimX* expression can be induced with IPTG at 1 mM.

2.4.8 | Competence With *Staphylococcus aureus*

Bacteria were cultured aerobically in tryptone soy agar at 37°C. A saturated culture of *S. aureus* USA300 (Boyle-Vavra et al. 2015) was adjusted to an OD₆₀₀ = 1, and 100 μL was spread onto a tryptic soy agar plate. A 5-μL suspension of *P. aeruginosa* PA14 or PA14Δ32 was spotted onto these plates, which were incubated overnight at 37°C. Inhibition halos, along with colony diameters, were measured using the ImageJ software (Fiji).

2.4.9 | Antibiotic Susceptibility Testing

Minimal inhibitory concentrations (MICs) were determined by using Sensititre plates (Thermo Fisher Scientific). *P. aeruginosa* PA14 and PA14Δ32 were cultured ON in LB at 37°C under aerobic conditions. These cultures were then used in antibiotic test panels by following the manufacturer's instructions. To do this, the OD₆₀₀ was diluted to a 0.5 McFarland scale, and 5 μL of the suspension was transferred to commercial Mueller-Hinton broth adjusted for cation concentration. A 50-μL aliquot of this suspension was then added to each well of the Sensititre plate. The inoculated plates were incubated ON at 37°C, and bacterial growth was determined in each well.

2.4.10 | Bacterial Growth Profile on Different Carbon Sources

Single colonies of the strains under study were used to inoculate precultures, grown in the same medium and conditions used for subsequent growth monitoring. Precultures were incubated for 24 h. For growth monitoring, 200 μL of medium was inoculated with the corresponding preculture to an OD₆₀₀ = 0.02 and dispensed into a 96-well plate. The cultures were incubated at 37°C in a Synergy HI plate reader (BioTek Instruments Inc.), and OD₆₀₀ was recorded every 15 min. Media tested included M9 minimal medium supplemented with 10 mM citrate, gluconate, glycerol, succinate, or succinate (Volke et al. 2021), as well as LB.

2.4.11 | Bacterial Tolerance to Stress Conditions

Single colonies of the specified strains were used to inoculate precultures, which were grown for 24 h. Growth was monitored in 1 mL of the corresponding medium, inoculated with the preculture to an OD₆₀₀ = 0.02 and dispensed into a 96-well plate. Cultures were incubated at 37°C in a Synergy HI plate reader (BioTek Instruments Inc.), with OD₆₀₀ measured every 15 min. pH tolerance was evaluated using LB adjusted to a pH range of 6–10, with phosphate buffer for pH=6–9 and glycine phosphate buffer for pH=10. Saline stress was assessed using LB

containing NaCl concentrations up to 1 M. Oxidative stress analysis involved aerobic cultures in tryptic soy agar at 37°C, followed by spreading 100 µL of culture onto LB agar plates. Filter disks embedded with 10 µL of H₂O₂ were placed on the plates, and after overnight incubation at 37°C, inhibition halos and colony diameters were measured using the ImageJ software (Fiji).

2.5 | Determination of c-di-GMP Levels Through a Transcriptional Biosensor and Analytical Quantification by LC–MS/MS

A fluorescence-based transcriptional biosensor, comprising the monomeric green fluorescent protein (msfGFP) gene regulated by the *P_{pelA}* promoter (Baraquet et al. 2012), was integrated as a Tn7 module into the chromosome of *P. aeruginosa* PA14 and PA14Δ32 by tetraparental mating (Benedetti et al. 2016). For this, *E. coli* PIR2 (Thermo Fisher Scientific) carrying plasmid pBG-PelA or pBG-PelA-Sm (donor strain), *E. coli* DH5α *λpir* carrying plasmid pTnS1 (helper strain expressing the transposase), *E. coli* HB101 carrying plasmid pRK600 (helper strain), and *P. aeruginosa* (recipient strain) were mixed in LB, streaked on LB agar plates, and incubated at 37°C for 24 h (Ruiz et al. 2006; Federici et al. 2025). *P. aeruginosa* clones carrying *attTn7::[P_{pelA}(BCD2)→msfGFP]* chromosomal integrations were selected on cetrimide agar plates containing gentamicin and confirmed by colony PCR (Choi et al. 2005). These clones were stored as glycerol stocks, streaked on LB agar plates, and four colonies were grown in M9 minimal medium for 16 h at 37°C under the conditions specified in the text. After washing with 1× PBS and standardising to OD₆₀₀=1, fluorescence was measured using a Synergy HT microtiter plate reader (BioTek Instruments Inc.).

ON cultures of both PA14 and PA14Δ32 strains were prepared in 10 mL of LB at 37°C with shaking at 200 rpm. Antibiotics were supplemented as needed to maintain plasmids during the experiments. The following day, 20 mL of LB was inoculated to an OD₆₀₀=0.05 with the ON cultures and placed in a 100-mL Erlenmeyer flask. When the OD₆₀₀ reached 0.5, the cultures were centrifuged at 4,000×g for 5 min at 4°C (Wirth et al. 2022). The supernatant was discarded, and the cell pellet was quenched with 2 mL of a solution containing 40% (v/v) acetonitrile and 40% (v/v) methanol in water, acidified with 0.1 M formic acid. After vigorous vortexing, cell debris was removed by centrifugation at 13,000×g for 2 min. The supernatant was transferred to a fresh tube and concentrated to 0.1 mL at 30°C for 2–3 h using an Eppendorf Concentrator Plus (Sigma-Aldrich Co.). The analysis of c-di-GMP was performed via LC–MS/MS as previously described (Volke, Gurdo et al. 2023; Volke, Orsi et al. 2023). Detection parameters, optimised for c-di-GMP quantification, are provided in Table S3.

2.6 | Transcriptomic Analysis

Strains were cultivated according to the protocol for c-di-GMP quantification. Once cultures reached an OD₆₀₀=0.5, cells from 2 mL of culture were harvested by centrifugation at 4,000×g for 5 min at 4°C. The resulting cell pellets were flash-frozen in liquid nitrogen and stored at –80°C for subsequent analysis. RNA extraction was performed as described by Turlin et al. (2023), and RNA quality was evaluated using an Agilent

2100 Bioanalyzer (RNA 6000 Nano kit; Agilent Technologies, Waldbronn, Germany), assessing RNA concentration, RNA integrity number, 28S/18S ratio, and fragment length distribution. Library construction, sequence filtering, mapping, and genome expression analysis were outsourced to BGI Genomics Co. (Hong Kong). Protein–protein interaction network and enrichment analyses of differentially expressed genes were conducted using the *STRING* web platform (<https://string-db.org/>; Szklarczyk et al. 2018).

2.7 | Data and Statistical Analysis

All the experiments were independently repeated at least twice, as indicated in the corresponding figure or table legend, and the mean value of the corresponding parameter ± standard deviation is presented unless otherwise indicated. When relevant, the level of significance of the differences when comparing results was evaluated by ANOVA and Tukey multiple comparison test or Student's *t*-test with $\alpha=0.05$.

3 | Results

3.1 | Construction of a *P. aeruginosa* Strain With Disrupted GCPs

P. aeruginosa possesses one of the most complex c-di-GMP signalling networks among bacteria, with 40 proteins containing DGC or PDE domains. Our primary objective was to generate a *P. aeruginosa* strain in which all c-di-GMP–metabolising proteins were inactivated. To achieve this goal, we adopted a multiplex CRISPR/Cas base-editing system previously developed for *Pseudomonas* species in our laboratory (Volke et al. 2022), which enables the simultaneous inactivation of multiple genes (Figure 1A). This system expresses multiple gRNAs under a single promoter, which are post-transcriptionally processed by the endoribonuclease Cas6f into mature gRNAs with distinct spacers (Figure 1B). A CRISPR/Cas complex fused to a cytidine base editor (CBE) catalyses cytidine-to-thymine conversions that are permanently incorporated into the genome during DNA replication. We targeted 32 proteins predicted to contain a DGC domain (GGDEF or similar) in *P. aeruginosa* PA14 (Figure 2 and Table S4). Spacers were designed to target locations within the corresponding open reading frames (ORFs) to disrupt GCP genes, following established criteria (Volke et al. 2022). These criteria required the editable cytidine to be positioned between the second and tenth positions within the editing window, while avoiding guanosine residues immediately preceding the editable cytidine (Table S5). By applying these criteria, all GCP-encoding ORFs distributed across the *P. aeruginosa* chromosome were successfully edited, achieving 100% base-editing efficiency.

P. aeruginosa DGC proteins typically have a GGDEF domain at the C-terminus, while in most dual GGDEF/EAL-domain proteins, the GGDEF domain is followed by the EAL domain near the C-terminus (Figure 2). This arrangement enabled the introduction of premature *STOP* codons in the ORF of each gene upstream of the GGDEF motif (Figure 2). The ORFs PA14_31330 and PA14_69900, predicted to encode dual EAL-GGDEF

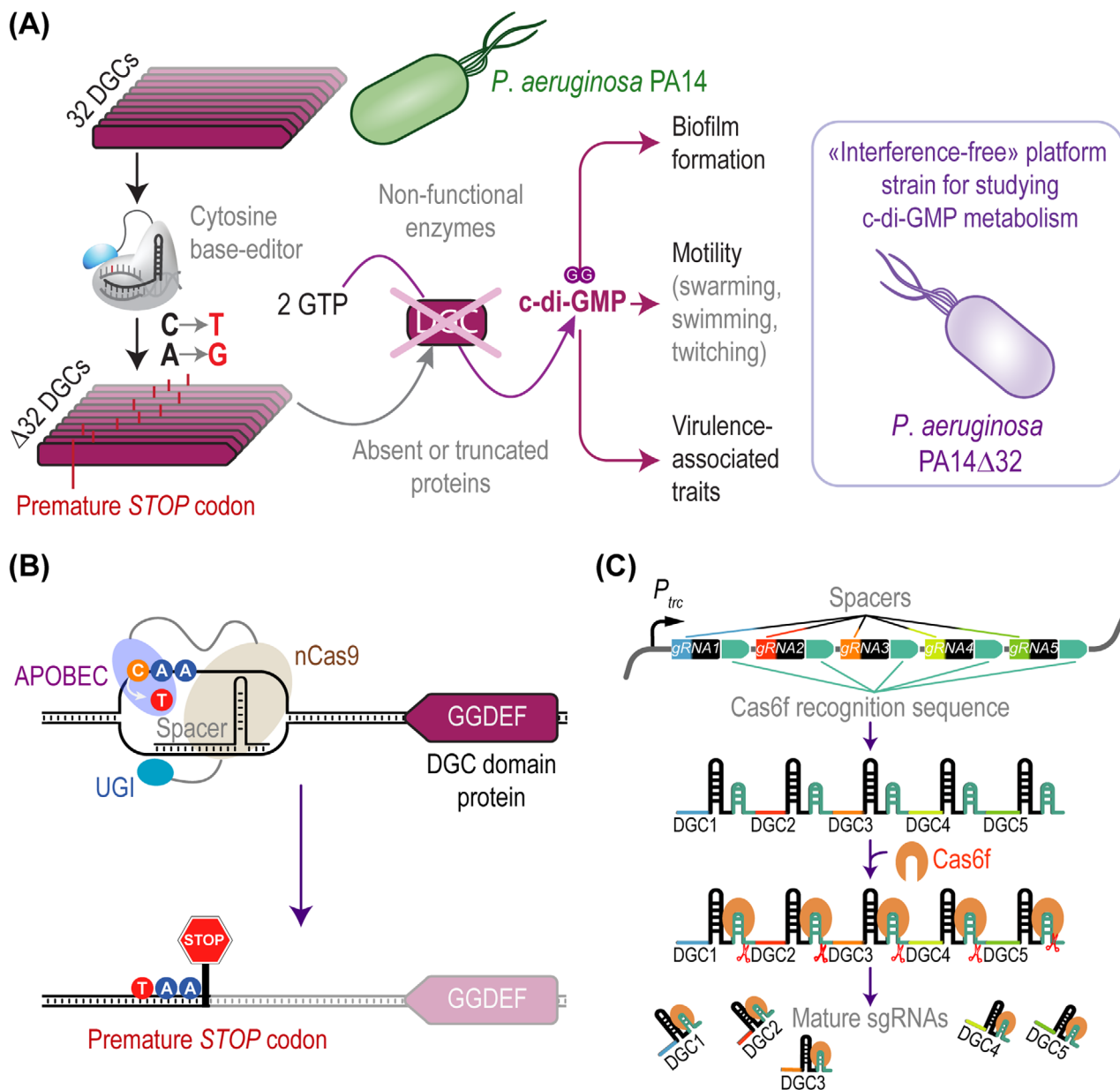


FIGURE 1 | Overall strategy for constructing a *P. aeruginosa* strain disrupted in GGDEF-containing proteins. (A) All 32 diguanylate cyclase (DGC)-encoding genes of *P. aeruginosa* PA14 were interrupted by introducing premature *STOP* codons using a multiplexed cytosine base-editor. The synthesis of c-di-GMP, a key regulator of biofilm formation, motility, and virulence-associated phenotypes, was severely impaired in the resulting strain lacking all 32 DGCs (*P. aeruginosa* PAΔ32). This «interference-free» strain provides a platform to study the isolated effects of enzymes involved in c-di-GMP turnover. (B) Cytosine base-editor structure. A nicking Cas9 (nCas9), guided by a single guide RNA (sgRNA), targets the cognate protospacer sequence. Upon hybridization between the single guide RNA (sgRNA) spacer and the target DNA, the complementary strand is exposed. A cytidine deaminase (APOBEC, from *Rattus norvegicus*) fused to nCas9 deaminates cytosine (C) to uracil within an editing window, and during DNA replication, uridine is converted to thymidine (T). The uracil DNA glycosylase inhibitor (UGI) prevents cytosine restoration by endogenous DNA repair pathways. Spacers are designed to induce a premature *STOP* codon through the C-to-T exchange within the DGC coding sequence. (C) RNA cassette processing by Cas6f. The individual sgRNA spacers, cloned in pBEC/pMBEC vectors and targeting the different DGC genes (Table S1), include a 3' recognition site for the endoribonuclease Cas6f, which cuts the polycistronic RNA and remains bound to each sgRNA post-cleavage.

proteins previously identified as phosphodiesterases rather than diguanylate cyclases (Rao et al. 2009; Feng et al. 2020), were modified by partially interrupting the GGDEF domain with *STOP* codons. For PA14_21870, the only protein where the EAL domain is N-terminal to the GGDEF motif, the target cytidine residue was situated between the two domains. In a few other cases (PA14_04420, PA14_07500, and PA14_64050), the ORFs contained more than one targeted cytidine residue.

Derivatives of the base-editing pBEC/pMBEC vectors (Volke et al. 2022) carrying the required gRNAs to modify all 32 targets were assembled (Table S1) and introduced into *P. aeruginosa* PA14 through iterative editing cycles (Figure S1A). After each cycle, colony PCR was performed on randomly selected isolates, and amplicon sequencing confirmed successful edits, enabling the selection of partial mutants for subsequent rounds of base-editing. When a given spacer proved inefficient at

PA14 locus tag	Name	Gene length (bp)	Protein length (amino acids)	Activity	Swimming	Swarming	Twitching	Protein structure
02110	<i>siaD</i>	708	236	DGC	—	— —		
03720	<i>pipA</i>	2,283	761	PDE	—		+	
03790		972	324	DGC		— —	— —	
04420		1,131	377	N.D.		— —	—	
07500	<i>rncA</i>	3,738	1,246	PDE	— —	—		
16500	<i>wspR</i>	1,044	348	DGC	+	+		
20820	<i>hsbD</i>	1,170	390	DGC			+	
21190	<i>nbdA</i>	2,358	786	PDE	— —	—	—	
21870		1,806	602	PDE	++		—	
23130		924	308	DGC	+	—	—	
26970		1,578	526	DGC	—	— —	— —	
31330		1,500	500	PDE	—		—	
37690		2,595	865	PDE	—		+	
40570		1,206	402	DGC			—	
42220	<i>mucR</i>	2,058	686	DGC-PDE	++	++		
45930	<i>lapD</i>	1,953	651	DD				
49160		3,363	1,121	DGC			—	
49890	<i>yfiN</i>	1,308	436	DGC	+	+		
50060	<i>roeA</i>	1,197	399	DGC		+		
53140	<i>rbdA</i>	2,472	824	PDE		—		
53310		2,046	682	DGC		+		
56280	<i>sadC</i>	1,128	376	DGC	+		—	
56790	<i>bifA</i>	2,064	688	PDE	— —	—	—	
57140		1,101	367	N.D.		—	—	
60870	<i>morA</i>	4,248	1,416	PDE	— —	—		
64050	<i>gcbA</i>	1,629	543	DGC		+	—	
65090	<i>nicD</i>	2,022	674	DGC				
65540	<i>fimX</i>	2,076	692	PDE	++	++	—	
66320	<i>dipA</i>	2,700	900	PDE	— —	—		
69900	<i>proE</i>	1,677	559	PDE			—	
71850		2,853	951	N.D.	— —		—	
72420	<i>dgcH</i>	2,016	672	DGC	—	— —	— —	

FIGURE 2 | Structure and characteristics of GCPs in *P. aeruginosa* PA14. The GGDEF-containing protein (GCP) architecture and position of premature *STOP* codons generated by base-editing are shown for each GCP in *P. aeruginosa* PA14. Protein structures are not drawn to scale. Data on DGC activity, swimming, swarming, and twitching were obtained from Ha and O'Toole (2015) and Kulasakara et al. (2006); see also Table S4. The symbols (+, ++, —, — —) reflect the degree of motility changes observed in single GCP mutants as reported by Ha et al. (2014). Empty boxes indicate no discernible motility effect. *Abbreviations*: GGDEF, canonical diguanylate cyclase domain; EAL, phosphodiesterase domain; PAS, signal transduction domain; TM, inner membrane transmembrane domain; SBD, periplasmic substrate-binding domain; REC, response regulator domain; MHYT, integral membrane protein domain; CBS, cystathionine β -synthase domain; GAF-like, c-di-GMP-specific phosphodiesterases, adenylyl cyclases, and FhlA domain; CHASE4 and CHASE8, periplasmic sensor domains; HAMP, histidine kinases, adenylyl cyclases, methyl binding proteins, phosphatases; LapD/MoxY periplasmic, N-terminal periplasmic domain of the LapD and MoxY receptor proteins; 7TM-DISM, signal transduction domain with seven transmembrane receptors with diverse intracellular signalling modules; DD, degenerate GGDEF and EAL/HD-GYP domain considered non-functional for c-di-GMP synthesis or degradation; N.D., not experimentally determined.

editing its target gene, alternative spacer designs were tested and implemented (Table S2). By the end of this iterative base-editing process, whole-genome sequencing verified the successful editing of all 32 targets. This genome-engineering effort produced *P. aeruginosa* PA14Δ32, a mutant strain in which all known c-di-GMP-synthesizing enzymes (i.e., *wspR*, *yfiN*, *morA*, PA14_72420, *rbdA*, *bifA*, PA14_71850, PA14_50060, PA14_53310, PA14_65090, PA14_20820, PA14_26970, PA14_40570, PA14_21870, PA14_31330, PA14_37690, PA14_45930, PA14_65540, PA14_03720, PA14_69900, PA14_04420, PA14_23130, PA14_02110, PA14_03790, PA14_42220, PA14_49160, PA14_66320, PA14_21190, PA14_07500, PA14_57140, PA14_56280, and PA14_64050; Table S1 and Figure S1B) were disrupted.

3.2 | *P. aeruginosa* PA14Δ32 Exhibits Stable Physiology Across Growth Conditions Despite Substantially Decreased c-di-GMP Levels

The PA14Δ32 mutant displayed a plateau-like colony morphology with plaque-like clearing zones at the centres, contrasting with the regular colony phenotype of the wild-type strain on LB agar (Figure 3A). Growth rates in complex and minimal media supplemented with various carbon and energy sources were lower than those of the parental strain under all tested conditions (Figure 3B). However, the extent of this reduction suggests a relatively limited disruption to the overall bacterial physiology due to the lack of DGC proteins. The most pronounced growth rate decrease (ca. 35%) was observed in cultures containing gluconeogenic substrates, while cultures in LB exhibited only a slight reduction (ca. 14%) compared to the wild-type strain. Furthermore, strain PA14Δ32 was more sensitive to oxidative stress, as evidenced by larger inhibition halos following H₂O₂ exposure (Figure 3C). This increased sensitivity probably results from the loss of key c-di-GMP-metabolising enzymes that promote biofilm formation and enhance oxidative stress defences. In *P. aeruginosa*, oxidative stress typically triggers an increase in c-di-GMP levels via the activation of specific DGCs (e.g., PA14_23130 and PA3177) and the suppression of certain PDEs. In contrast, no significant differences were observed in responses to variations in pH (Figure S2A) or osmolarity (Figure S2B), tested in the presence of NaCl (Danchin and Nikel 2019).

Intracellular c-di-GMP levels were semi-quantitatively assessed using a c-di-GMP-responsive fluorescent biosensor (Benedetti et al. 2016). This system places the gene encoding msfGFP under the transcriptional control of the c-di-GMP-responsive *P_{pelA}* promoter from *P. aeruginosa* (Figure 3D). In its native context, this promoter regulates the expression of the *pel* operon, involved in exopolysaccharide biosynthesis (Vasseur et al. 2005). The biosensor-based measurements revealed c-di-GMP levels barely above the background in the PA14Δ32 strain (Figure 3D). LC-MS/MS-based c-di-GMP quantification revealed significantly reduced (>80%) dinucleotide concentrations in cell extracts of *P. aeruginosa* PA14Δ32 (Figure 3E)—a more accurate estimation due to the lower detection limit of LC-MS/MS compared to fluorescence-based biosensors. These results suggest that some targeted enzymes may retain partial activity or

that cryptic pathways contribute to c-di-GMP synthesis in the PA14Δ32 background. Based on these observations, we focused on characterising this *P. aeruginosa* mutant with markedly reduced c-di-GMP levels.

3.3 | Differentially Expressed Genes Upon GCPs Disruption in Strain PA14Δ32

To examine the impact of GCP disruption on gene expression, we performed a genome-wide transcriptomic analysis using deep RNA sequencing on exponentially growing cultures of strain PA14Δ32 grown in LB. Differential gene expression was identified by setting thresholds of log₂ of the fold-change (FC) > 2 or < −2 as an indication of transcriptional up- or down-regulation, respectively. The analysis revealed significant alterations in the transcription of 225 genes in strain PA14Δ32 compared to the parental strain, representing 4% of the gene repertoire of *P. aeruginosa*. Among these, 85% (192 genes) showed down-regulation, with log₂(FC) values < −2, while 15% (33 genes) were up-regulated. Detailed transcriptional changes are listed in Table S6, and a volcano plot summarising the data is presented in Figure 4A.

None of the disrupted GCPs showed significant changes in transcription, except for PA14_21190 (Table S7), which displayed a modest perturbation with a log₂(FC) = −2. To investigate the biological functions or metabolic pathways impacted by GCP disruption, we analysed differentially expressed genes using the *STRING* database (Szklarczyk et al. 2018). A protein–protein interaction network was constructed based on physical interactions and functional associations derived from curated sources, including Kyoto Encyclopedia of Genes and Genomes (KEGG) pathways (Kanehisa et al. 2022). In this network, the differentially expressed genes were organised into four primary clusters, all comprising downregulated genes (Figure 4B). These clusters included (i) phenazine biosynthesis and quorum sensing, (ii) siderophore metabolism and biosynthesis, (iii) protein secretion via the type VI secretion system and biofilm formation, and (iv) protein secretion via the type III secretion system and negative regulation of secretion (Data S1). Together, these clusters accounted for 53% of the downregulated functions and 45% of all differentially expressed genes. Notably, they aligned with five metabolic pathways affected by the transcriptionally downregulated genes in strain PA14Δ32: biofilm formation, phenazine biosynthesis, quorum sensing, bacterial secretion systems, and siderophore and non-ribosomal peptide biosynthesis (Figure 4C and Data S1). The most significant transcriptional changes occurred in phenazine and siderophore biosynthesis, with 60% and 86% of pathway genes, respectively, being down-regulated. Analysis of off-target mutations revealed no changes in genes associated with these metabolic pathways (Data S2). We found that the transcription of 29 quorum sensing-related genes, including *rhlR* that encodes a key transcriptional regulator, were significantly repressed in the mutant (Figure S3). Taken together, these findings demonstrate that disrupting GCP in *P. aeruginosa*, which reduces c-di-GMP levels, significantly attenuates key mechanisms governing biofilm formation and virulence. The experimental validation of the transcriptional analysis results is detailed below.

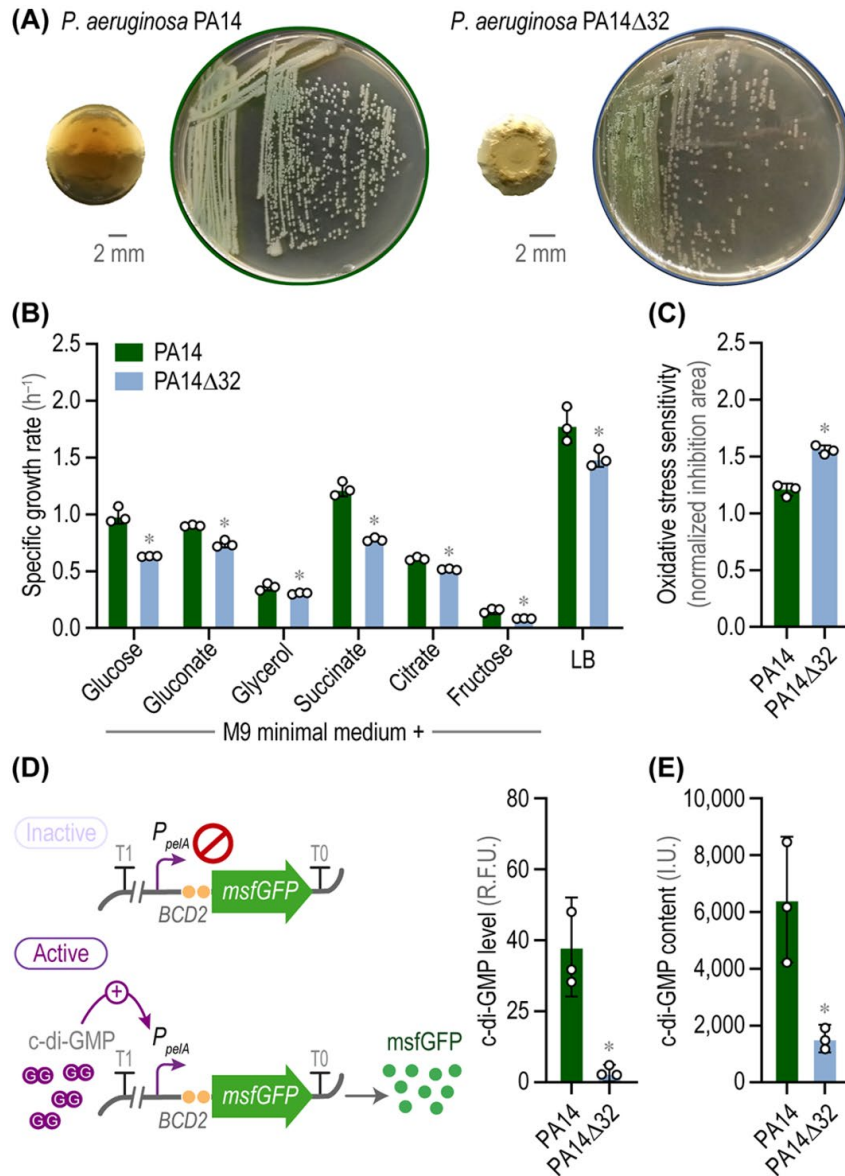


FIGURE 3 | *P. aeruginosa* PA14Δ32 maintains consistent physiology across growth conditions despite substantially reduced c-di-GMP levels. (A) Colony morphology and streak plate images of strains PA14 and PA14Δ32. LB agar plates were incubated for 24 h at 37°C and photographed under bright-field illumination. (B) Specific growth rates of *P. aeruginosa* PA14 and PA14Δ32 growing on various carbon sources. Cultures were inoculated in either LB or M9 minimal medium supplemented with different carbon substrates and grown at 37°C with agitation. (C) Oxidative stress sensitivity assays. Bacteria were cultured in tryptic soy medium, spread on LB agar plates, and exposed to H₂O₂ in filter-paper disks embedded with 10 μL of H₂O₂. Inhibition halos and bacterial colonies diameter were measured after overnight incubation at 37°C. Results represent average values ± standard deviation from three independent experiments. (D) A transcriptional biosensor for assessing c-di-GMP levels in vivo. The monomeric and superfolder green fluorescent protein (*msfGFP*) is under transcriptional control of the c-di-GMP-responsive *P_{pelA}* promoter from the *P. aeruginosa pel* operon. Strains carrying the biosensor were cultured in M9 minimal medium supplemented with glucose and acid casein hydrolysate for 24 h and standardised to the same optical density at 600 nm (OD₆₀₀). Results represent the mean relative fluorescence units (R.F.U.) ± standard deviations from triplicate measurements from at least two independent experiments. (E) c-di-GMP levels quantified via LC-MS/MS. Cultures of both strains were grown in LB and adjusted to the same OD₆₀₀. Results represent the average c-di-GMP level (in arbitrary intensity units, I.U.) ± standard deviations relative to wild-type *P. aeruginosa* PA14, based on three independent experiments. In all cases, statistical significance with *p* < 0.05 is indicated by an asterisk (*) symbol (Student's *t*-test).

3.4 | Biofilm Formation Is Suppressed in Strain PA14Δ32

c-di-GMP is a critical regulator of biofilm formation, with elevated intracellular levels linked to sessile cells and increased biofilm production (Ha and O'Toole 2015). Biofilm formation

was assessed using the standard crystal violet staining (CVS) method (Navarro et al. 2011) to compare the wild-type strain with the PA14Δ32 mutant. The wild-type strain had an average biofilm index of 0.5 ± 0.2 , reflecting robust biofilm formation (Figure 5A,B). In contrast, the PA14Δ32 mutant exhibited no detectable biofilm formation under these conditions.

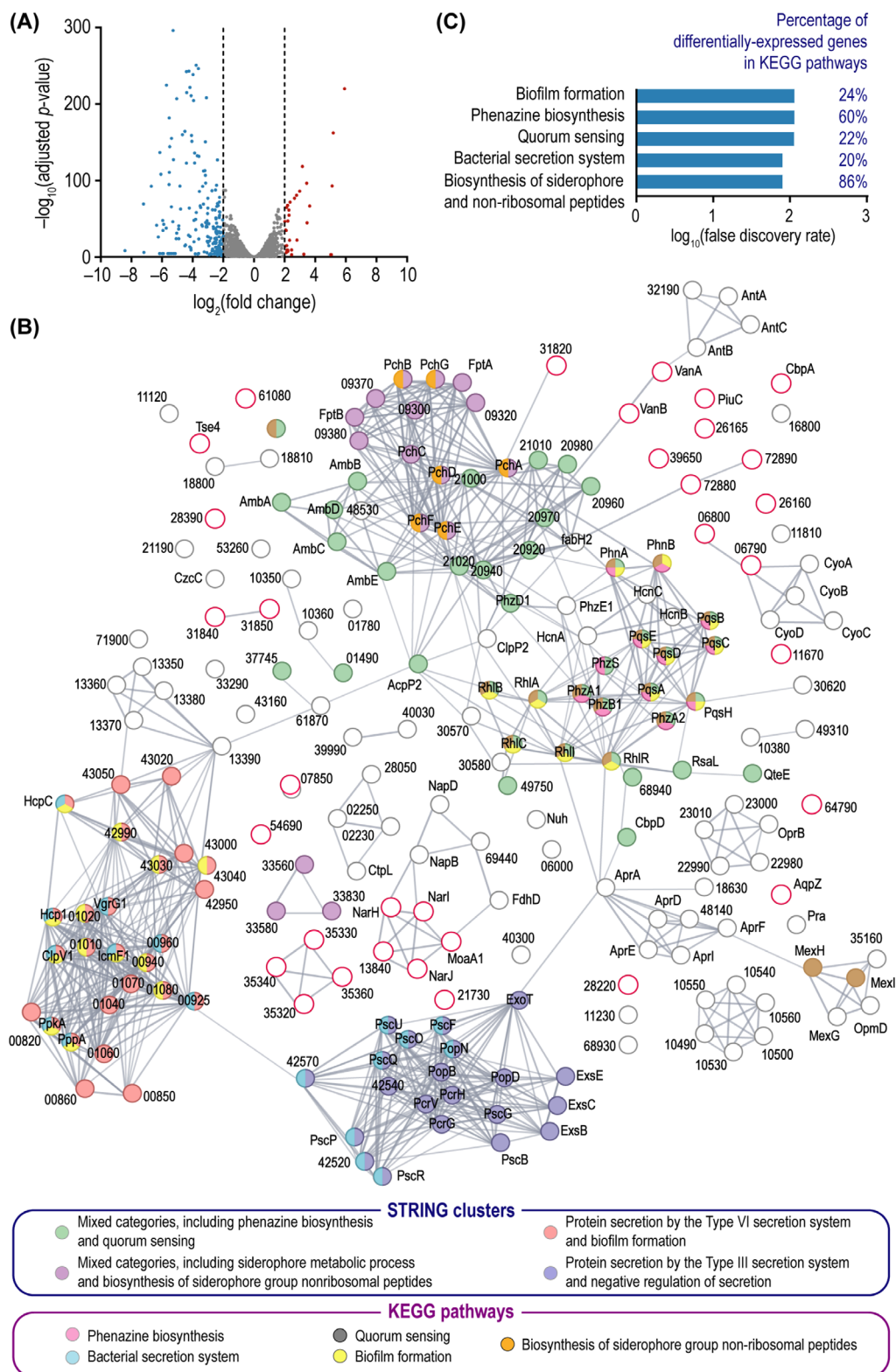


FIGURE 4 | Differentially expressed genes upon GCPs disruption. *P. aeruginosa* PA14 and PA14Δ32 strains were cultured with agitation at 37°C until mid-exponential phase ($OD_{600}=0.5$). Cells were harvested for RNA sequencing to identify differentially expressed genes in strain PA14Δ32. Genes with $p < 0.05$ and a $\log_2(\text{fold-change}) \geq 2$ (upregulated) or ≤ -2 (downregulated) compared to wild-type *P. aeruginosa* PA14 were selected. (A) Volcano plot of differentially expressed genes identified by RNA sequencing. Blue and red dots represent downregulated and upregulated genes, respectively. (B) Protein-protein interaction network of differentially expressed genes, constructed using the *STRING* web tool (Szklarczyk et al. 2018). Clusters were organised based on protein interactions and their roles in specific cellular processes. Red-lined circles indicate upregulated genes, with PA14 loci labelled by their specific numbers. (C) Kyoto Encyclopedia of Genes and Genomes (KEGG) pathway enrichment analysis of differentially expressed genes. False discovery rates describe pathway enrichment significance; values for multiple testing were corrected using the Benjamini-Hochberg procedure as implemented in the *STRING* web tool.

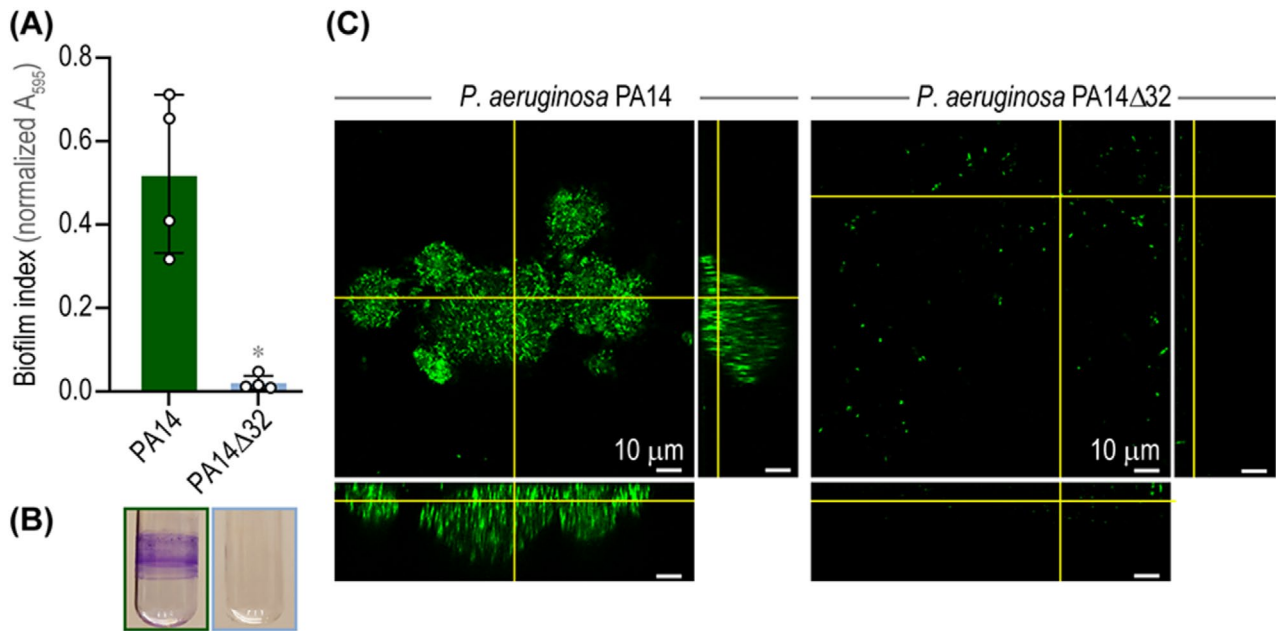


FIGURE 5 | Biofilm formation is abolished in strain PA14Δ32. (A) Biofilm formation by *P. aeruginosa* PA14 and PA14Δ32 quantified after 24 h of growth at 37°C in polystyrene microtiter plates under static conditions. The extent of biofilm formation was assessed by measuring the absorbance at 595 nm (A_{595} , normalised by the biomass in each well) following crystal violet staining and elution with ethanol. Results represent averages \pm standard deviations from quadruplicate measurements in at least three independent experiments. Statistical significance with $p < 0.05$ is indicated by an asterisk (*) symbol (Student's *t*-test). (B) Images of crystal violet-stained biofilms of *P. aeruginosa* PA14 and PA14Δ32 after overnight growth in LB at 37°C with agitation. (C) Confocal laser scanning microscopy of biofilm structures in strains PA14 and PA14Δ32 after 24 h of growth in 8-well Lab-Tek chamber slides stained with SYTO 9. Images are representative of four observations from at least two independent experiments.

Confocal laser scanning microscopy showed that the PA14Δ32 mutant lacks a defined biofilm structure, while the wild-type strain formed a well-organised biofilm. Biofilm formation by strain PA14Δ32 was virtually suppressed, with only sparse surface-attached bacteria observed in the preparation (Figure 5C). These findings support the conclusion that GCP proteins orchestrate the shift from planktonic to multicellular lifestyles in *P. aeruginosa* but are not essential for cell viability. Additionally, the minimal c-di-GMP levels detected in the mutant (<20% of those in the parental strain) appear insufficient to support biofilm production. Building on these observations, we explored other phenotypic traits potentially affected by altered c-di-GMP metabolism.

3.5 | The GCP-Disrupted Mutant Maintains Normal Swimming but Lacks Swarming and Twitching Motility

P. aeruginosa uses two surface structures, a single polar monotrichous flagellum and polar type IV pili, to facilitate movement. These organelles enable three distinct motility types: (i) swimming in liquid environments, driven by the flagellum, (ii) twitching across solid surfaces through pilus extension and retraction, and (iii) swarming on semisolid surfaces, which depends on flagellar stators and rhamnolipid production (Caiazza et al. 2005). The relationship between c-di-GMP levels and motility involves complex interactions (Simm et al. 2004). Mutations in enzymes regulating c-di-GMP turnover lead to varying effects on motility, from enhancement to complete

movement inhibition (Ha and O'Toole 2015). Based on this background, the next objective was to examine motility in the PA14Δ32 mutant.

The PA14Δ32 mutant retained swimming motility comparable to the wild type (Figure 6A), indicating that disrupting GCPs does not significantly impact flagellum assembly or function. However, *P. aeruginosa* PA14Δ32 exhibited no swarming or twitching motility (Figure 6B,C), suggesting that one or more GGDEF-domain proteins are crucial for these specific behaviours. Transmission electron microscopy (TEM) confirmed the presence of a polar flagellum in strain PA14Δ32, structurally resembling the wild type (Figure 6D). Notably, transcription of the structural *rhl* genes, which encode key components involved in rhamnolipid production (RhlA, RhlB, and RhlC), was significantly downregulated in the mutant (Table S6)—accounting for the swarming deficiency. Additionally, the inactivation of *fimX* (PA14_65540), a dual-domain GGDEF-EAL protein critical for type IV pilus biogenesis and assembly (Kazmierczak et al. 2006), helps explain the observed twitching failure. In this sense, the gene encoding FimX was the final base-edit during strain construction (Figure S1A), allowing its function to be tested independently of the other 31 GGDEF-domain proteins. This mutant strain, termed *P. aeruginosa* PA14Δ31 (Table S1), displayed normal twitching motility and pili (Figure 6C,D), comparable to the wild type. Complementation of *fimX* in the PA14Δ32 background with plasmid pMBLe_ *fimX* restored both twitching motility and normal piliation levels (Figure 6C,D)—similar to the observations in the wild-type strain and the PA14Δ31 mutant.

Taken together, these findings highlight the critical role of FimX among GGDEF-domain proteins in supporting twitching motility. Remarkably, twitching persisted even with significantly reduced c-di-GMP levels. These results prompted further experiments to assess whether the phenotypic changes in the GCP-depleted strain could impact virulence.

3.6 | Strain PA14Δ32 Has Reduced Production of Virulence Factors, While Its Antibiotic Resistance Profile Remains Unaffected

Virulence traits in *P. aeruginosa* are tightly regulated by different GCPs through modulation of c-di-GMP levels (Kulasakara et al. 2006). Transcriptomic analysis of the PA14Δ32 strain revealed a marked downregulation of key components in both the *rhl* (*rhlABC*, *rhlI*, and *rhlR*) and the *pqsABCDEH* systems (Table S6), which collectively orchestrate quorum sensing. In turn, quorum sensing coordinates diverse physiological processes, including biofilm formation, and regulates the production of various virulence factors (Papenfort and Bassler 2016). To evaluate the impact of GCP disruption on virulence traits, assays were performed to measure key virulence traits such as extracellular proteases, rhamnolipids, and pigments.

Production of the siderophore pyoverdine (Figure 7A) and the phenazine pyocyanin (Figure 7B) was significantly reduced in strain PA14Δ32, with levels <13% and 1%, respectively, compared to the wild-type strain. Additionally, the mutant exhibited impaired rhamnolipid production (Figure 7C) and decreased extracellular protease (exoprotease) activity (Figure 7D), with reductions of ca. 80% and 40%, respectively. These findings align with low expression of the *rhlABC* genes involved in rhamnolipid biosynthesis. Significant transcriptional changes were also observed in *phzABCDE* and *pchABCDEFG*, genes responsible for pyocyanin and pyoverdine synthesis (Table S6 and Data S1). Reduced exoprotease production correlated with transcriptional downregulation of genes involved in secretion systems, particularly type III and type IV systems (Figure 7D, Table S6 and Data S1).

Antibiotic resistance is potentially influenced by c-di-GMP levels (Gupta et al. 2014; Nicastro et al. 2014). To investigate this aspect, we determined the minimum inhibitory concentration (MIC) of the PA14Δ32 mutant and compared it with the wild-type strain using a panel of clinically relevant antibiotics, including ceftazidime, amikacin, and gentamicin. *P. aeruginosa* PA14Δ32 exhibited resistance levels comparable to the wild-type strain across nearly all antibiotics tested (Table S8). These molecular insights into virulence were further examined in a dual bacterial infection model, as described below.

3.7 | Reduced Virulence and Diminished Competitiveness Against *Staphylococcus aureus* Following GCP Disruption

In cystic fibrosis and chronically infected wounds, *P. aeruginosa* and *Staphylococcus aureus* often coexist as comorbid human pathogens. Pyocyanin-mediated inter- and intracellular signalling allows *P. aeruginosa* to outcompete *S. aureus*, providing a

clear competitive advantage (Biswas et al. 2009; Hotterbeekx et al. 2017). Additionally, *P. aeruginosa* may utilise exoproteases to compete with staphylococci and sequester iron from *S. aureus* via the iron-chelating molecule pyoverdine (Mashburn et al. 2005; Biswas et al. 2009).

Given the observed impairment in extracellular virulence factors upon elimination of GGDEF-domain proteins (Figure 7 and Table S6), we investigated how altered c-di-GMP levels influence interspecies competition with *S. aureus*. In co-culture assays, *P. aeruginosa* PA14Δ32 exhibited a significant 1.3-fold reduction in inhibitory activity against *S. aureus* strain USA300 compared to the wild-type strain (Figure 7E). These findings, once again, underscore the importance of c-di-GMP in modulating interspecies interactions, a key aspect of virulence. To further explore the pathogenicity profile of the PA14Δ32 mutant, the free-living nematode *Caenorhabditis elegans* was used as a model organism (Mahajan-Miklos et al. 1999). A paralysis assay was performed to compare the effects of the wild-type strain and the PA14Δ32 mutant on adult worms exposed to bacterial lawns grown on brain-heart agar. The PA14Δ32 mutant had markedly reduced virulence; ca. 98% of the worms survived after 6 h, similar to the negative control with *E. coli* OP50 cells (Figure 7F). In contrast, only ca. 16% of worms survived exposure to the wild-type strain (Figure 7F). Taken together, these results highlight the essential role of c-di-GMP in regulating virulence and pathogenesis in *P. aeruginosa*. The next set of experiments was designed to correlate these phenotypes with key GGDEF-domain proteins.

3.8 | Genetic Complementation of Strain PA14Δ32 With Specific GGDEF-Domain Proteins Partially Restores Wild-Type Phenotypes

Two GGDEF-domain proteins, WspR and PA14_23130, were selected for complementation in both the wild-type strain and the PA14Δ32 mutant to investigate the broader effects of altered c-di-GMP levels beyond GCP-specific influences (Figure 8). WspR, a key component of the *P. aeruginosa* wrinkly spreader phenotype (Wsp) chemosensory system (Figure 8A), is one of the most active DGCs in this species (Kulasakara et al. 2006). This system detects surface-induced cell envelope stress, promoting a biofilm lifestyle via c-di-GMP signalling (Luo et al. 2015; O'Neal et al. 2022). In the PA14 strain, PA14_23130 is homologous to PA3177 of *P. aeruginosa* PAO1, which encodes an active DGC associated with biofilm drug tolerance (Table S4). However, its role in attachment and biofilm formation remains unclear (Poudyal and Sauer 2018). These proteins were chosen for their cytoplasmic localization because they are GGDEF-only variants, involved in diverse cellular processes (Table S4).

Expression of *wspR* and *PA14_23130* in strain PA14Δ32 resulted in increased c-di-GMP content compared to the wild-type, with *wspR* expression producing the highest levels, supporting its role in c-di-GMP synthesis (Figure 8B). Expression of *wspR* in PA14Δ32 and wild-type strains induced a small-colony variant (SCV) phenotype and fully restored biofilm formation in PA14Δ32 (Figure 8C,E). Confocal microscopy confirmed the development of comparably structured, densely packed biofilms in both the wild type and PA14Δ32 expressing

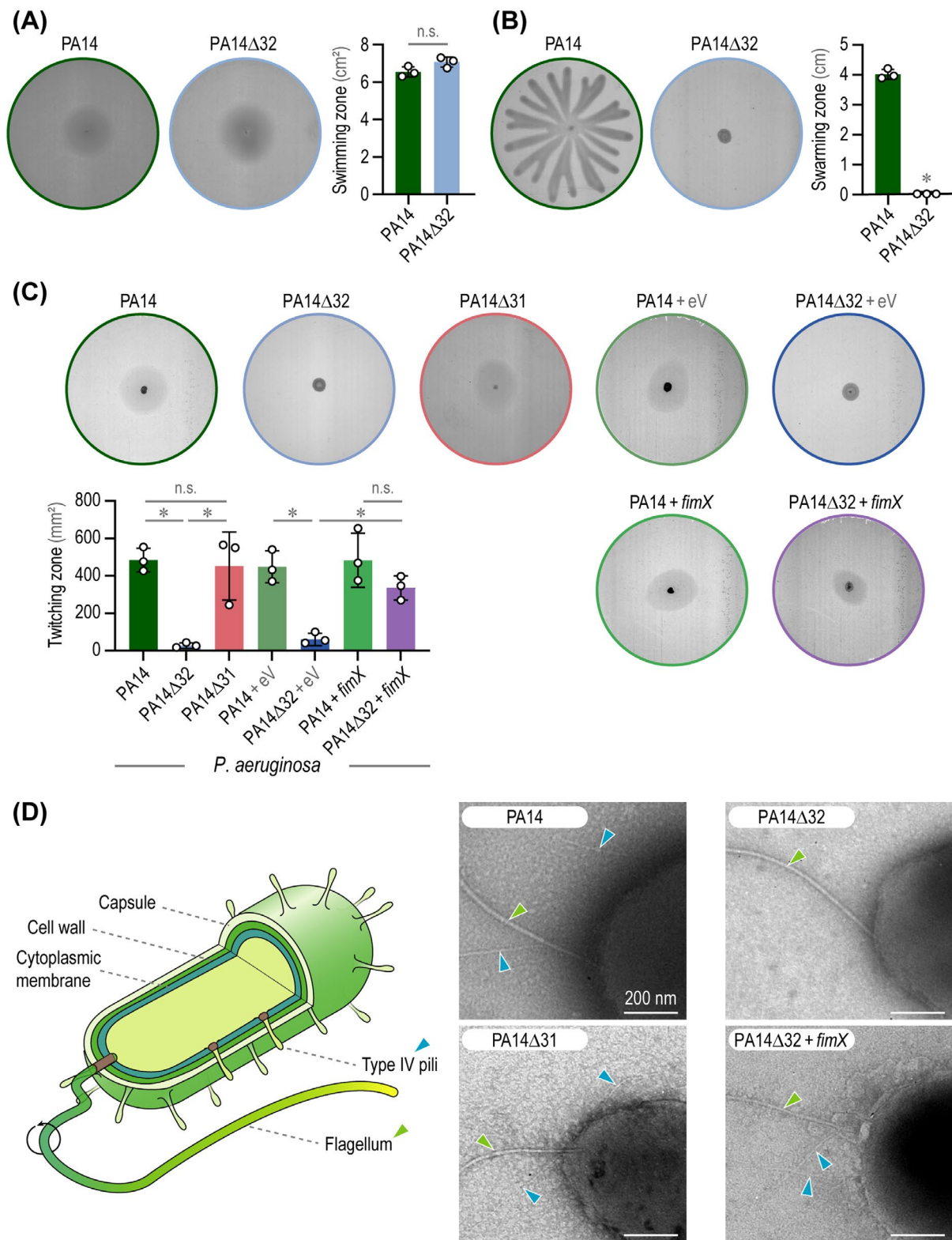


FIGURE 6 | The GCP-disrupted mutant maintains normal swimming but lacks swarming and twitching motility. Analysis of (A) swimming and (B) swarming motility in *P. aeruginosa* PA14 and PA14Δ32. (C) Twitching motility in strains PA14, PA14Δ31, and PA14Δ32, and their derivatives transformed with plasmids pMBLe (empty vector, eV, used as a control) or pMBLe_ *fimX* (+ *fimX*). Results in panels (A), (B), and (C) represent averages \pm standard deviations from quadruplicate measurements across three independent experiments. Statistically significant differences ($p < 0.05$) were determined with the Student's *t*-test; the asterisk (*) symbol indicates significance for swarming, *n.s.* indicates no significant differences for swimming. Levels of significance in twitching motility were assessed using one-way ANOVA followed by Tukey's post hoc test, with the asterisk (*) symbol denoting significance at $p < 0.05$. (D) Scheme of a *P. aeruginosa* cell showing the flagellum and pili, accompanied by transmission electron microscopy images used to visualise surface pili and flagella in strains PA14, PA14Δ32, PA14Δ31, and PA14Δ32 + *fimX*. Light blue and light green arrowheads indicate pili and flagella, respectively.

wspR, rescuing the biofilm deficiency in the multiple mutant (Figure 5C). *PA14_23130* expression in the wild-type background did not affect biofilm formation, consistent with previous reports (Poudyal and Sauer 2018). However, in the PA14Δ32 mutant, *PA14_23130* expression induced biofilm formation and SCV phenotypes (Figure 8C–E).

To evaluate antibiotic resistance, the PA14Δ32 mutant engineered to express *PA14_23130* (referred to as PA14Δ32 + 23130) was tested against the same antibiotic panel described above

(Table S8). Strain PA14Δ32 + 23130 showed resistance levels similar to those of the wild-type strain and the PA14Δ32 mutant for nearly all antibiotics tested, diverging from earlier reports. Notably, the absence of 31 GGDEF-domain proteins allowed this DGC to promote biofilm formation comparable to that observed with highly active *wspR* expression (Figure 8D,E). Although SCVs are generally associated with higher antibiotic resistance due to robust biofilm formation, the MIC assays reported in our study were performed on planktonic cultures. This experimental setup explains why the PA14Δ32 mutant expressing *PA14_23130*

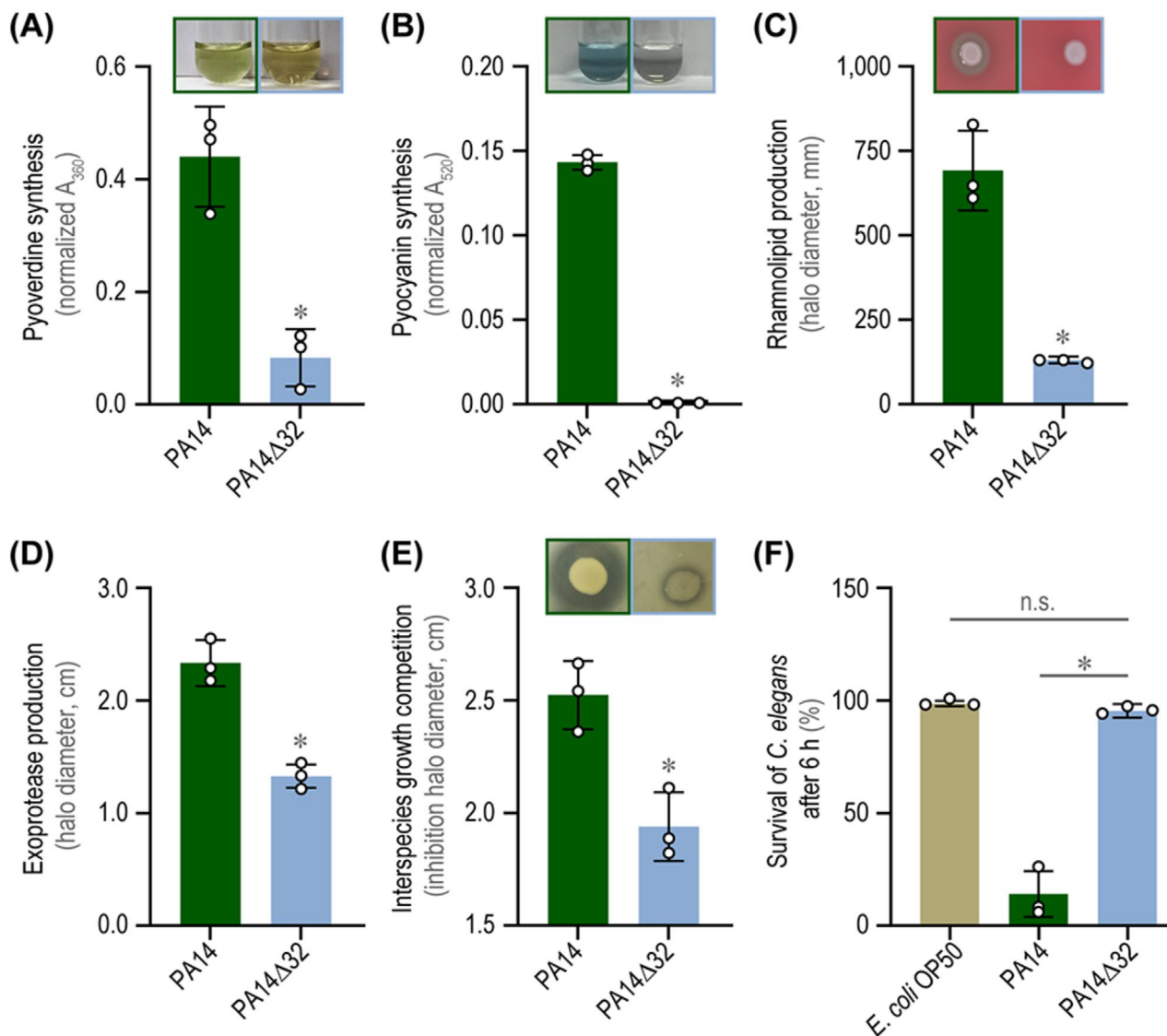


FIGURE 7 | Virulence-associated traits in *P. aeruginosa* PA14Δ32. (A) Pyoverdine quantification from King's B culture supernatants, measured by absorbance at 360 nm (A_{360} , normalised by cell density). (B) Pyocyanin extraction from LB culture supernatants using chloroform, quantified by absorbance at 520 nm (A_{520} , normalised by cell density). (C) Rhamnolipid production assessed via hemolysis on sheep blood agar; 5 μ L of bacterial culture was spotted and incubated at 37°C for 96 h. (D) Exoprotease activity determined by proteolytic halos on 1% (w/v) milk agar after incubation at 37°C overnight. (E) Competition between *P. aeruginosa* and *S. aureus* USA300 assessed on tryptic soy agar plates. *S. aureus* cultures ($OD_{600} = 1$) were spread, and a 5- μ L spot of PA14 or PA14Δ32 cultures was added; inhibition halos and colony diameters were measured after overnight incubation. (F) Paralysis assay with *C. elegans* exposed to *P. aeruginosa* strains grown on brain-heart infusion agar. Halo and colony diameters in panels (C), (D), and (E) were analysed using the ImageJ software. Statistical significance at $p < 0.05$ is marked by an asterisk (*) symbol; non-significant differences are denoted as n.s. (Student's *t*-test). In all cases, results represent averages \pm standard deviations of triplicate or quadruplicate measurements from three independent experiments.

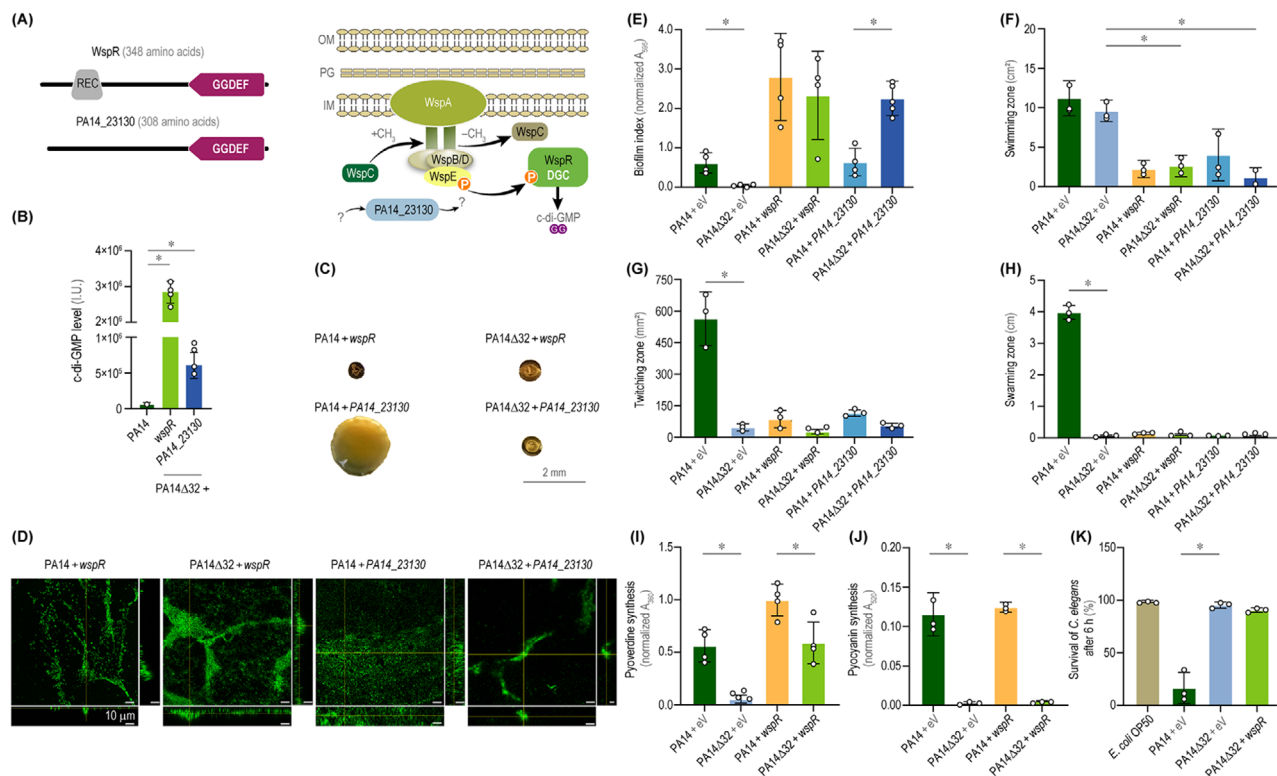


FIGURE 8 | Complementation of strain PA14Δ32 with specific GGDEF-domain proteins partially restores wild-type phenotypes. (A) Domain architecture of the cytoplasmic DGCs WspR and PA14_23130, both featuring the GGDEF domain, with WspR additionally containing a phosphoreceiver (REC) domain. The Wsp signal transduction complex comprises six proteins: WspA, an inner membrane (IM) receptor detecting surface-induced activation signals; WspE, which phosphorylates WspR, leading to c-di-GMP synthesis; WspC (methyltransferase) and WspF (methyl-erase), which mediate signal transduction through methyl (CH₃) group transfers; and WspB and WspD, scaffold proteins ensuring proper complex localization and function (O'Connor et al. 2012). Abbreviations: OM, outer membrane; PG, peptidoglycan; and GGDEF, diguanylate cyclase domain. (B) LC-MS/MS analysis of c-di-GMP levels in *P. aeruginosa* PA14Δ32 expressing *wspR* or PA14_23130 as compared to *P. aeruginosa* PA14. Cultures were grown in LB supplemented with 0.1% (w/v) arabinose and normalised to the same OD₆₀₀ before analysis. Results represent average c-di-GMP level (in arbitrary intensity units, I.U.) ± standard deviations. Characterisation of (C) colony morphology, (D) confocal laser scanning microscopy of biofilm structures in *P. aeruginosa* PA14 and PA14Δ32 strains expressing *wspR* or PA14_23130, (E) biofilm formation, (F) swimming, (G) twitching, (H) swarming, (I) pyoverdine synthesis, (J) pyocyanin synthesis, and (K) *C. elegans* paralysis assays. Experimental conditions for each assay were consistent with those described in previous figures. For all complementation assays, strains PA14 and PA14Δ32 carried the corresponding empty vector (eV) as a control. Measurements were performed in triplicate or quadruplicate across at least three independent experiments; results represent averages ± standard deviations. Statistical significance at $p < 0.05$ is indicated by an asterisk (*) symbol (one-way ANOVA with Tukey's *post hoc* test).

exhibited resistance levels similar to those of the wild-type and PA14Δ32 strains.

While the analysis of motility produced the results anticipated (Figure 8F–H), pigment production followed an unexpected pattern. Expression of *wspR* in strain PA14Δ32 restored pyoverdine to wild-type levels (Figure 8I), but pyocyanin production remained deficient (Figure 8J), suggesting that other GGDEF-domain proteins with distinct functions are critical for this phenotype. The reduced virulence of the PA14Δ32 mutant, assessed via *C. elegans* paralysis assays, was unaffected by *wspR* expression (Figure 8K), indicating that this DGC does not play a significant role in pathogenicity within this infection model.

4 | Discussion

In this study, we adopted a modular CRISPR/Cas9-based editing system (Volke et al. 2022) to disrupt the 32 GCP-encoding genes in *P. aeruginosa* PA14. Our approach overcame previous

challenges in genome editing for this bacterium, enabling the creation of a GCP-disrupted strain as a foundation for studying c-di-GMP signalling and metabolism. By introducing premature STOP codons into these genes, we examined the broader functional consequences of GCP disruption, with a focus on biofilm formation, motility, virulence, and antibiotic resistance profiles. As a general conclusion, and despite disrupting all 32 ORFs, the PA14Δ32 mutant exhibited viability and growth patterns within the range of the wild-type strain across various carbon sources—indicating that c-di-GMP synthesis is non-essential for basic cellular functions. The interplay between c-di-GMP levels and carbon metabolism in *P. aeruginosa* warrants further investigation, as studies in *E. coli*, *V. cholerae*, and *S. typhimurium* have revealed significant links between the second messenger and cell physiology. In *V. cholerae*, for instance, glucose-mediated interactions inactivate PdeS, increasing c-di-GMP levels and promoting biofilm formation (Heo et al. 2019). Similarly, some of the global regulators in *E. coli*, for example, CsrA, influence both carbon metabolism and c-di-GMP-regulated traits (Jonas et al. 2008). In *S. enterica*, high levels of c-di-GMP repress the

expression of genes involved in glucose (PTS^{Glucose}), mannose (PTS^{Mann}), and fructose (PTS^{Fructose}) uptake, guiding sugar metabolism to exopolysaccharide production (Baek and Yoon 2023). Transcriptional analysis in our study highlighted downregulation of some genes, for example, *oprB*, *gltK*, and ABC sugar transporter permease genes, possibly connecting c-di-GMP signalling to the uptake of glucose, glycerol, and fructose.

The residual c-di-GMP levels detected in *P. aeruginosa* PA14Δ32 suggest the existence of additional synthesis pathways or cryptic functions encoding dinucleotide-processing functions (Dahlstrom et al. 2018; Waters 2018; Borlee et al. 2022), which, in turn, underscores the complexity of c-di-GMP signalling characteristic of environmental bacteria. Complementation of the mutant with individual DGCs revealed phenotypes that expose roles beyond regulating c-di-GMP synthesis. For instance, reintroducing WspR in the mutant background partially restored biofilm formation and motility—suggesting that c-di-GMP levels alone do not dictate these traits and that specific GCP functions are needed for restoring wild-type-like phenotypes. These insights provide a framework to investigate individual DGC mechanisms in a system devoid of DGC redundancy, where the effect of single enzymes involved in c-di-GMP metabolism can be studied while avoiding crosstalk with similar functions. We previously applied a similar experimental framework by constructing a mutant of *P. putida* devoid of all major NADP⁺-dependent dehydrogenases (Volke et al. 2022), where native and heterologous enzymes reducing the nucleotide can be characterised in growth-coupled designs (Fernández-Cabezón et al. 2019; Orsi et al. 2021, 2024; Gurdo et al. 2023).

The model associating biofilm formation with reduced motility was supported by swimming behaviour in experiments with the PA14Δ32 mutant, yet swarming and twitching deficiencies highlight additional complexity layers related to high c-di-GMP levels. Swarming, requiring flagellar function and rhamnolipid biosurfactants (Déziel et al. 2003; Caiazza et al. 2005; Tremblay et al. 2007), is probably impacted by disrupted biosurfactant production in strain PA14Δ32. Previous studies implicated GGDEF-domain proteins in motility-related functions (Toutain et al. 2005; Baker et al. 2019), suggesting their potential involvement in the regulation of swarming functions (including HsbD, NbdA, RoeA, SadC, BifA, GcbA, DipA, PA14_37690, and PA14_53310, all of which had altered transcription levels in the PA14Δ32 mutant). Comparative analyses with other bacteria, for example, *Salmonella* (Solano et al. 2009) and *Caulobacter crescentus* (Abel et al. 2013), demonstrate diverse motility phenotypes in GCP-deficient strains (Table S9), emphasising species-specific mechanisms. *D. zeae*, for instance, exhibited increased flagellum-mediated motility upon removal of GCPs (Chen et al. 2020), while motility was not affected in a similar mutant of *S. meliloti* (Schäper et al. 2016).

To explore individual DGCs and their interactions, we employed an “all-but-one” disruption strategy, leaving only FimX intact in strain PA14Δ31. *P. aeruginosa* PA14Δ31 had normal twitching and exhibited properly assembled type IV pili. Indeed, the introduction of FimX in the PA14Δ32 strain restored twitching and pili assembly, largely recapitulating the wild-type and PA14Δ31 phenotypes. Previous studies indicated that the degenerated GGDEF/EAL domains of FimX prevent c-di-GMP synthesis

or degradation (Kulasakara et al. 2006; Navarro et al. 2009). Instead, the PDE domain of this protein interacts with c-di-GMP, positively regulating pili assembly (Jain et al. 2012, 2017). Our data further suggest that FimX can regulate twitching and pili assembly even in the absence of other GCPs—highlighting, once again, the value of a bacterial system devoid of DGC redundancy for this type of studies.

Transcriptomic analyses also revealed downregulation of quorum sensing and biofilm-related genes, reflecting an intricate relationship between c-di-GMP, quorum sensing, and virulence. Quorum sensing is intricately linked with signalling molecules, for example, c-di-GMP and c-AMP, which mediate complex information translation in bacteria (Papenfort and Bassler 2016). For instance, reduced c-di-GMP can upregulate the expression of the *rhl* and *pqs* genes, linked to regulators such as PqsR (Lin Chua et al. 2017). However, the correlation between c-di-GMP levels, GGDEF-domain proteins, and quorum sensing-mediated virulence factor expression remains poorly understood. In fact, comparing different cyclase-deficient strains (Table S9) reveals that the roles of c-di-GMP and DGCs in biofilm formation and virulence vary across bacteria. Each species has unique regulatory pathways and factors influencing c-di-GMP-related phenotypes (Solano et al. 2009; Abel et al. 2013; Schäper et al. 2016; Chen et al. 2020). This diversity challenges the notion of a universal mechanism and emphasises the importance of considering species-specific traits in studying biofilm formation and virulence.

Our results further expose a reciprocal relationship between c-di-GMP levels and virulence, where elevated c-di-GMP levels suppress virulence factors—consistent with previous observations in *E. coli*, *S. enterica*, and *V. cholerae* (Kuchma et al. 2005; Tischler and Camilli 2005; Kulasakara et al. 2006; Moscoso et al. 2011; Chua et al. 2014). The PA14Δ32 strain had reduced fitness in interspecies competition with *S. aureus*—two pathogens commonly coexisting and competing in clinical setups (DeLeon et al. 2014; Alves et al. 2018; Briaud et al. 2019). This phenotype could be linked to decreased production of anti-staphylococcal virulence factors, for example, pyocyanin, a key virulence factor and a quorum sensing-signalling molecule (Jayaseelan et al. 2014). FliA, the alternative σ factor required for flagellin synthesis, influences pyocyanin production via c-di-GMP and BifA (Lo et al. 2016). Pyocyanin binds to RmcA, activating its phosphodiesterase activity (Okegbe et al. 2017), while BrlR functions as a receptor for both c-di-GMP and pyocyanin (Wang et al. 2018). While *wspR* expression *in trans* restored pyoverdine levels in *P. aeruginosa* PA14Δ32, pyocyanin production remained significantly low. This observation indicates that merely increasing c-di-GMP levels alone is insufficient for pyocyanin synthesis, suggesting the involvement of additional DGCs beyond WspR. The extensive repertoire of DGCs in *P. aeruginosa* reflects the need to sense and respond to a wide range of environmental and host-derived signals. As Dahlstrom and O'Toole (2017) elegantly described in their *symphony of cyclases* model, individual DGCs may contribute either to a global c-di-GMP pool or to discrete, localised signalling microdomains, thereby conferring specificity to distinct cellular responses. Our finding that WspR only partially rescues the phenotype in *P. aeruginosa* PA14Δ32 reinforces the notion that specific GCPs perform specialised, non-redundant functions in

modulating complex behaviours, for example, biofilm formation, motility, and virulence. These results are consistent with the recent study of Feng et al. (2025), who demonstrated that the ProE phosphodiesterase interacts directly with the quorum sensing protein PqsE to promote pyocyanin production in *P. aeruginosa*. These results highlight the importance of localised c-di-GMP degradation and specific protein–protein interactions in regulating quorum sensing-dependent virulence factor expression, thereby supporting the notion that distinct GCP-mediated pathways—rather than global c-di-GMP levels alone—are critical for key phenotypes. These findings also support the notion that c-di-GMP signalling operates in a localised or compartmentalised manner (Gilles-González and Sousa 2019; Nicastro et al. 2020). In the future, identifying the specific DGCs contributing to pyocyanin synthesis will contribute to our understanding of this intricate regulatory pathway—an effort supported by the availability of a bacterial system devoid of DGC redundancy.

The value of an “interference-free” bacterial system for dissecting individual enzymes or functions is illustrated by our experiments with *PA14_23130* expression. Poudyal and Sauer (2018) highlighted a role for the PA3177 cyclase (similar to the PA14_23130 protein) as a c-di-GMP modulator that influences biofilm drug tolerance. Comparable biofilm architectures in the wild-type strain and the Δ PA3177 mutant indicated a negligible impact of PA3177 on biofilm formation (Poudyal and Sauer 2018). Stempel et al. (2017) proposed that PA3177 plays a role in the HClO-induced stress response, affecting motility, biofilm formation, and macrophage interaction. In our study, expressing *PA14_23130*, the orthologue of PA3177 present in strain PA14, in the wild-type background did not affect biofilm production or architecture. However, *PA14_23130* expression in the “interference-free” PA14 Δ 32 background significantly influenced biofilm formation, suggesting a role for this DGC that could not be detected in the wild-type context. Hence, the genetic dissection approach adopted in our study offers a robust framework for addressing unresolved questions connected to the complex c-di-GMP signalling in *P. aeruginosa*, a model bacterial pathogen.

Author Contributions

Román A. Martino: conceptualization, investigation, methodology, writing – original draft. **Daniel C. Volke:** conceptualization, investigation, methodology, validation. **Albano H. Tenaglia:** investigation, methodology. **Paula M. Tribelli:** investigation, methodology. **Pablo I. Nikel:** conceptualization, funding acquisition, writing – review and editing, supervision, project administration. **Andrea M. Smania:** supervision, project administration, writing – review and editing, funding acquisition, conceptualization.

Acknowledgements

Andrea M. Smania is financially supported by the Agencia Nacional de Promoción Científica y Tecnológica (ANPCyT) through grant PICT-2019-1590, the Consejo Nacional de Investigaciones Científicas y Técnicas (CONICET) through grant PIP-2022-11220210100945CO, and the Secretaría de Ciencia y Tecnología de la Universidad Nacional de Córdoba (SECYT-UNC) through grant 33620180100413CB. Pablo I. Nikel gratefully acknowledges financial support from The Novo Nordisk Foundation through grants NNF20CC0035580, *LiFe*

(NNF18OC0034818), *TARGET* (NNF21OC0067996), *FM-Pseudomonas* (NNF24OC0091501), and *NovoF* (NNF23OC0083631), and the European Union's Horizon2020 Research and Innovation Programme under grant agreements Nos. 814418 (*SinFonia*) and 101082049 (*TOLERATE*). Román A. Martino received support from a postdoctoral fellowship from ANPCyT and Consejo Nacional de Ciencia y Tecnología (CONICET), as well as a Research and Training Grant from the Federation of European Microbiological Societies (FEMS). The responsibility for the content of this article rests solely with the authors, and the funding sources are not responsible for any use that may be made of the information contained therein.

Conflicts of Interest

The authors declare no conflicts of interest.

Data Availability Statement

Data supporting the findings of this study can be found in the paper and its Supporting Information. The WGS and the RNA-seq raw data generated in this study for the PA14 Δ 32 strain have been deposited in the public database GenBank under the BioProject ID PRJNA987335, which can be accessed at <https://www.ncbi.nlm.nih.gov/bioproject/>. Any additional data can be made available from the authors upon reasonable request. Materials can be made available upon reasonable request to the corresponding authors under a material transfer agreement.

References

- Abel, S., T. Bucher, M. Nicollier, et al. 2013. “Bi-Modal Distribution of the Second Messenger c-di-GMP Controls Cell Fate and Asymmetry During the *Caulobacter* Cell Cycle.” *PLoS Genetics* 9: e1003744.
- Alves, P. M., E. Al-Badi, C. Withycombe, P. M. Jones, K. J. Purdy, and S. E. Maddocks. 2018. “Interaction Between *Staphylococcus aureus* and *Pseudomonas aeruginosa* Is Beneficial for Colonisation and Pathogenicity in a Mixed Biofilm.” *Pathogens and Disease* 76: fty003.
- Baek, J., and H. Yoon. 2023. “Cyclic di-GMP Modulates a Metabolic Flux for Carbon Utilization in *Salmonella enterica* Serovar *Typhimurium*.” *Microbiology Spectrum* 11: e03685-22.
- Baker, A. E., S. S. Webster, A. Diepold, et al. 2019. “Flagellar Stators Stimulate c-di-GMP Production by *Pseudomonas aeruginosa*.” *Journal of Bacteriology* 201: e00741-18.
- Baraquet, C., K. Murakami, M. R. Parsek, and C. S. Harwood. 2012. “The FleQ Protein From *Pseudomonas aeruginosa* Functions as Both a Repressor and an Activator to Control Gene Expression from the *Pel* Operon Promoter in Response to c-di-GMP.” *Nucleic Acids Research* 40: 7207–7218.
- Benedetti, I., V. de Lorenzo, and P. I. Nikel. 2016. “Genetic Programming of Catalytic *Pseudomonas putida* Biofilms for Boosting Biodegradation of Haloalkanes.” *Metabolic Engineering* 33: 109–118.
- Bird, J. E., J. Marles-Wright, and A. Giachino. 2022. “A user's Guide to Golden Gate Cloning Methods and Standards.” *ACS Synthetic Biology* 11: 3551–3563.
- Biswas, L., R. Biswas, M. Schlag, R. Bertram, and F. Götz. 2009. “Small-Colony Variant Selection as a Survival Strategy for *Staphylococcus aureus* in the Presence of *Pseudomonas aeruginosa*.” *Applied and Environmental Microbiology* 75: 6910–6912.
- Blin, K., L. E. Pedersen, T. Weber, and S. Y. Lee. 2016. “CRISpy-Web: An Online Resource to Design sgRNAs for CRISPR Applications.” *Synthetic and Systems Biotechnology* 1: 118–121.
- Bobrov, A. G., O. Kirillina, D. A. Ryjenkov, et al. 2011. “Systematic Analysis of Cyclic di-GMP Signalling Enzymes and Their Role in Biofilm Formation and Virulence in *Yersinia pestis*.” *Molecular Microbiology* 79: 533–551.

- Borlee, G. I., M. R. Mangalea, K. H. Martin, B. A. Plumley, S. J. Golon, and B. R. Borlee. 2022. "Disruption of c-di-GMP Signaling Networks Unlocks Cryptic Expression of Secondary Metabolites During Biofilm Growth in *Burkholderia pseudomallei*." *Applied and Environmental Microbiology* 88: e02431-21.
- Boyle-Vavra, S., X. Li, M. T. Alam, et al. 2015. "USA300 and USA500 Clonal Lineages of *Staphylococcus aureus* do Not Produce a Capsular Polysaccharide due to Conserved Mutations in the *cap5* Locus." *mBio* 6: e02585-14.
- Briaud, P., L. Camus, S. Bastien, A. Doléans-Jordheim, F. Vandenesch, and K. Moreau. 2019. "Coexistence with *Pseudomonas aeruginosa* Alters *Staphylococcus aureus* Transcriptome, Antibiotic Resistance and Internalization Into Epithelial Cells." *Scientific Reports* 9: 16564.
- Brinkman, F. S. L., G. L. Winsor, R. E. Done, et al. 2021. "The *Pseudomonas aeruginosa* Whole Genome Sequence: A 20th Anniversary Celebration." *Advances in Microbial Physiology* 79: 25–88.
- Caiazza, N. C., R. M. Shanks, and G. A. O'Toole. 2005. "Rhamnolipids Modulate Swarming Motility Patterns of *Pseudomonas aeruginosa*." *Journal of Bacteriology* 187: 7351–7361.
- Chen, Y., J. Zhou, M. Lv, Z. Liang, M. R. Parsek, and L. H. Zhang. 2020. "Systematic Analysis of c-di-GMP Signaling Mechanisms and Biological Functions in *Dickeya zeae* EC1." *mBio* 11: e02993-20.
- Choi, K. H., J. B. Gaynor, K. G. White, et al. 2005. "A Tn7-Based Broad-Range Bacterial Cloning and Expression System." *Nature Methods* 2: 443–448.
- Chua, S. L., Y. Liu, J. K. Yam, et al. 2014. "Dispersed Cells Represent a Distinct Stage in the Transition From Bacterial Biofilm to Planktonic Lifestyles." *Nature Communications* 5: 4462.
- Colque, C. A., A. G. Albarracín Orio, P. E. Tomatis, et al. 2022. "Longitudinal Evolution of the *Pseudomonas*-Derived Cephalosporinase (PDC) Structure and Activity in a Cystic Fibrosis Patient Treated With β -Lactams." *mBio* 13: e01663.
- Cordisco, E., and D. O. Serra. 2025. "Moonlighting Antibiotics: The Extra Job of Modulating Biofilm Formation." *Trends in Microbiology*, In Press. <https://doi.org/10.1016/j.tim.2024.12.011>.
- Costerton, J. W. 2001. "Cystic Fibrosis Pathogenesis and the Role of Biofilms in Persistent Infection." *Trends in Microbiology* 9: 50–52.
- Dahlstrom, K. M., A. J. Collins, G. Doing, et al. 2018. "A Multimodal Strategy Used by a Large c-di-GMP Network." *Journal of Bacteriology* 200: e00703-17.
- Dahlstrom, K. M., and G. A. O'Toole. 2017. "A Symphony of Cyclases: Specificity in Diguanylate Cyclase Signaling." *Annual Reviews of Microbiology* 71: 179–195.
- Danchin, A., and P. I. Nikel. 2019. "Why Nature Chose Potassium." *Journal of Molecular Evolution* 87: 271–288.
- DeLeon, S., A. Clinton, H. Fowler, J. Everett, A. R. Horswill, and K. P. Rumbaugh. 2014. "Synergistic Interactions of *Pseudomonas aeruginosa* and *Staphylococcus aureus* in an *in vitro* Wound Model." *Infection and Immunity* 82: 4718–4728.
- Déziel, E., F. Lépine, S. Milot, and R. Villemur. 2003. "*rhlA* Is Required for the Production of a Novel Biosurfactant Promoting Swarming Motility in *Pseudomonas aeruginosa*: 3-(3-Hydroxyalkanoyloxy)alkanoic Acids (HAAs), the Precursors of Rhamnolipids." *Microbiology* 149: 2005–2013.
- Eilers, K., J. Kuok Hoong Yam, R. Morton, et al. 2022. "Phenotypic and Integrated Analysis of a Comprehensive *Pseudomonas aeruginosa* PAO1 Library of Mutants Lacking Cyclic-di-GMP-Related Genes." *Frontiers in Microbiology* 13: 949597.
- Federici, F., F. Luppino, C. Aguilar-Vilar, et al. 2025. "CIFR (Clone-Integrate-Flip-Out-Repeat): A Toolset for Iterative Genome and Pathway Engineering of Gram-Negative bacteria." *Metabolic Engineering* 88: 180–195.
- Feng, Q., S. D. Ahator, T. Zhou, et al. 2020. "Regulation of Exopolysaccharide Production by ProE, a Cyclic-di-GMP Phosphodiesterase in *Pseudomonas aeruginosa* PAO1." *Frontiers in Microbiology* 11: 1226.
- Feng, Q., X. Dai, Q. Wu, L. Zhang, L. Yang, and Y. Fu. 2025. "C-di-GMP Phosphodiesterase ProE Interacts With Quorum Sensing Protein PqsE to Promote Pyocyanin Production in *Pseudomonas aeruginosa*." *mSphere* 10: e0102624.
- Fernández-Cabezón, L., A. Cros, and P. I. Nikel. 2019. "Evolutionary Approaches for Engineering Industrially-Relevant Phenotypes in Bacterial Cell Factories." *Biotechnology Journal* 14: 1800439.
- Fernández-Cabezón, L., A. Cros, and P. I. Nikel. 2021. "Spatiotemporal Manipulation of the Mismatch Repair System of *Pseudomonas putida* Accelerates Phenotype Emergence." *ACS Synthetic Biology* 10: 1214–1226.
- Galperin, M. Y., and S. H. Chou. 2022. "Sequence Conservation, Domain Architectures, and Phylogenetic Distribution of the HD-GYP Type c-di-GMP Phosphodiesterases." *Journal of Bacteriology* 204: e00561-19.
- Gilles-González, M.-A., and E. H. S. Sousa. 2019. "*Escherichia coli* DosC and DosP: A Role of c-di-GMP in Compartmentalized Sensing by Degradosomes." *Advances in Microbial Physiology* 75: 53–67.
- Gjermansen, M., P. Ragas, C. Sternberg, S. Molin, and T. Tolker-Nielsen. 2005. "Characterization of Starvation-Induced Dispersion in *Pseudomonas putida* Biofilms." *Environmental Microbiology* 7: 894–904.
- Gupta, K., J. Liao, O. E. Petrova, K. E. Cherny, and K. Sauer. 2014. "Elevated Levels of the Second Messenger c-di-GMP Contribute to Antimicrobial Resistance of *Pseudomonas aeruginosa*." *Molecular Microbiology* 92: 488–506.
- Curdo, N., D. C. Volke, D. McCloskey, and P. I. Nikel. 2023. "Automating the Design-Build-Test-Learn Cycle Towards Next-Generation Bacterial Cell Factories." *New Biotechnology* 74: 1–15.
- Ha, D. G., and G. A. O'Toole. 2015. "c-di-GMP and Its Effects on Biofilm Formation and Dispersion: A *Pseudomonas aeruginosa* Review." *Microbiology Spectrum* 3: 301–317.
- Ha, D. G., M. E. Richman, and G. A. O'Toole. 2014. "Deletion Mutant Library for Investigation of Functional Outputs of Cyclic Diguanylate Metabolism in *Pseudomonas aeruginosa* PA14." *Applied and Environmental Microbiology* 80: 3384–3393.
- Hengge, R. 2009. "Principles of c-di-GMP Signalling in bacteria." *Nature Reviews Microbiology* 7: 263–273.
- Hengge, R. 2021. "High-Specificity Local and Global c-di-GMP Signaling." *Trends in Microbiology* 29: 993–1003.
- Heo, K., Y. H. Park, K. A. Lee, et al. 2019. "Sugar-Mediated Regulation of a c-di-GMP Phosphodiesterase in *Vibrio cholerae*." *Nature Communications* 10: 5358.
- Hotterbeekx, A., S. Kumar-Singh, H. Goossens, and S. Malhotra-Kumar. 2017. "*In vivo* and *in vitro* Interactions Between *Pseudomonas aeruginosa* and *Staphylococcus* spp." *Frontiers in Cellular and Infection Microbiology* 7: 106.
- Jain, R., A. J. Behrens, V. Kaefer, and B. I. Kazmierczak. 2012. "Type IV Pilus Assembly in *Pseudomonas aeruginosa* Over a Broad Range of Cyclic di-GMP Concentrations." *Journal of Bacteriology* 194: 4285–4294.
- Jain, R., O. Sliusarenko, and B. I. Kazmierczak. 2017. "Interaction of the Cyclic-di-GMP Binding Protein FimX and the Type 4 Pilus Assembly ATPase Promotes Pilus Assembly." *PLoS Pathogens* 13: e1006594.
- Jayaseelan, S., D. Ramaswamy, and S. Dharmaraj. 2014. "Pyocyanin: Production, Applications, Challenges and New Insights." *World Journal of Microbiology and Biotechnology* 30: 1159–1168.
- Jenal, U., A. Reinders, and C. Lori. 2017. "Cyclic di-GMP: Second Messenger Extraordinaire." *Nature Reviews Microbiology* 15: 271–284.

- Jonas, K., A. N. Edwards, R. Simm, T. Romeo, U. Römling, and O. Meleforts. 2008. "The RNA Binding Protein CsrA Controls Cyclic di-GMP Metabolism by Directly Regulating the Expression of GGDEF Proteins." *Molecular Microbiology* 70: 236–257.
- Junkermeier, E. H., and R. Hengge. 2023. "Local Signaling Enhances Output Specificity of Bacterial c-di-GMP Signaling Networks." *MicroLife* 4: uqad026.
- Kanehisa, M., M. Furumichi, Y. Sato, M. Kawashima, and M. Ishiguro-Watanabe. 2022. "KEGG for Taxonomy-Based Analysis of Pathways and Genomes." *Nucleic Acids Research* 51: D587–D592.
- Kazmierczak, B. I., M. B. Lebron, and T. S. Murray. 2006. "Analysis of FimX, a Phosphodiesterase That Governs Twitching Motility in *Pseudomonas aeruginosa*." *Molecular Microbiology* 60: 1026–1043.
- Köhler, T., C. van Delden, L. K. Curty, M. M. Hamzehpour, and J. C. Pechere. 2001. "Overexpression of the MexEF-OprN Multidrug Efflux System Affects Cell-To-Cell Signaling in *Pseudomonas aeruginosa*." *Journal of Bacteriology* 183: 5213–5222.
- Kozaeva, E., Z. S. Nielsen, M. Nieto-Domínguez, and P. I. Nikel. 2024. "The pAbl-pCasso Self-Curing Vector Toolset for Unconstrained Cytidine and Adenine Base-Editing in Gram-Negative bacteria." *Nucleic Acids Research* 52: e19.
- Kozaeva, E., S. Volkova, M. R. A. Matos, et al. 2021. "Model-Guided Dynamic Control of Essential Metabolic Nodes Boosts Acetyl-Coenzyme A-Dependent Bioproduction in Rewired *Pseudomonas putida*." *Metabolic Engineering* 67: 373–386.
- Krink, N., P. I. Nikel, and C. L. Beisel. 2024. "A Hitchhiker's Guide to CRISPR Editing Tools in bacteria." *EMBO Reports* 25: 1694–1699.
- Kuchma, S. L., J. P. Connolly, and G. A. O'Toole. 2005. "A Three-Component Regulatory System Regulates Biofilm Maturation and Type III Secretion in *Pseudomonas aeruginosa*." *Journal of Bacteriology* 187: 1441–1454.
- Kulasakara, H., V. Lee, A. Brenic, et al. 2006. "Analysis of *Pseudomonas aeruginosa* Diguanylate Cyclases and Phosphodiesterases Reveals a Role for bis-(3'-5')-cyclic-GMP in Virulence." *Proceedings of the National Academy of Sciences of the United States of America* 103: 2839–2844.
- La Rosa, R., H. K. Johansen, and S. Molin. 2018. "Convergent Metabolic Specialization Through Distinct Evolutionary Paths in *Pseudomonas aeruginosa*." *mBio* 9: e00269-18.
- Liberati, N. T., J. M. Urbach, S. Miyata, et al. 2006. "An Ordered, Nonredundant Library of *Pseudomonas aeruginosa* Strain PA14 Transposon Insertion Mutants." *Proceedings of the National Academy of Sciences of the United States of America* 103: 2833–2838.
- Lin Chua, S., Y. Liu, Y. Li, et al. 2017. "Reduced Intracellular c-di-GMP Content Increases Expression of Quorum Sensing-Regulated Genes in *Pseudomonas aeruginosa*." *Frontiers in Cellular and Infection Microbiology* 7: 451.
- Lo, Y. L., L. Shen, C. H. Chang, M. Bhuwan, C. H. Chiu, and H. Y. Chang. 2016. "Regulation of Motility and Phenazine Pigment Production by FliA Is Cyclic-di-GMP Dependent in *Pseudomonas aeruginosa* PAO1." *PLoS One* 11: e0155397.
- Luján, A. M., M. D. Maciá, L. Yang, S. Molin, A. Oliver, and A. M. Smania. 2011. "Evolution and Adaptation in *Pseudomonas aeruginosa* Biofilms Driven by Mismatch Repair System-Deficient Mutators." *PLoS One* 6: e27842.
- Luján, A. M., A. J. Moyano, I. Segura, C. E. Argaraña, and A. M. Smania. 2007. "Quorum-Sensing-Deficient (*lasR*) Mutants Emerge at High Frequency From a *Pseudomonas aeruginosa mutS* Strain." *Microbiology* 153: 225–237.
- Luo, Y., K. Zhao, A. E. Baker, et al. 2015. "A Hierarchical Cascade of Second Messengers Regulates *Pseudomonas aeruginosa* Surface Behaviors." *mBio* 6: e02456-14.
- Macesic, N., A. C. Uhlemann, and A. Y. Peleg. 2025. "Multidrug-Resistant Gram-Negative Bacterial Infections." *Lancet* 405: 257–272.
- Mah, T. F., and G. A. O'Toole. 2001. "Mechanisms of Biofilm Resistance to Antimicrobial Agents." *Trends in Microbiology* 9: 34–39.
- Mahajan-Miklos, S., M. W. Tan, L. G. Rahme, and F. M. Ausubel. 1999. "Molecular Mechanisms of Bacterial Virulence Elucidated Using a *Pseudomonas aeruginosa*-*Caenorhabditis elegans* Pathogenesis Model." *Cell* 96: 47–56.
- Martínez-García, E., S. Fraile, E. Algar, et al. 2023. "SEVA 4.0: An Update of the Standard European Vector Architecture Database for Advanced Analysis and Programming of Bacterial Phenotypes." *Nucleic Acids Research* 51: D1558–D1567.
- Mashburn, L. M., A. M. Jett, D. R. Akins, and M. Whiteley. 2005. "*Staphylococcus aureus* Serves as an Iron Source for *Pseudomonas aeruginosa* During *in vivo* Coculture." *Journal of Bacteriology* 187: 554–566.
- Molinari, G., S. S. Ribeiro, K. Müller, et al. 2025. "Multiple Chaperone DnaK-FliC Flagellin Interactions Are Required for *Pseudomonas aeruginosa* Flagellum Assembly and Indicate a New Function for DnaK." *Microbial Biotechnology* 18: e70096.
- Moscato, J. A., H. Mikkelsen, S. Heeb, P. Williams, and A. Filloux. 2011. "The *Pseudomonas aeruginosa* Sensor RetS Switches Type III and Type VI Secretion via c-di-GMP Signalling." *Environmental Microbiology* 13: 3128–3138.
- Moyano, A. J., C. R. Mas, C. A. Colque, and A. M. Smania. 2020. "Dealing With Biofilms of *Pseudomonas aeruginosa* and *Staphylococcus aureus*: *In vitro* Evaluation of a Novel Aerosol Formulation of Silver Sulfadiazine." *Burns* 46: 128–135.
- Navarro, M. V., N. De, N. Bae, Q. Wang, and H. Sondermann. 2009. "Structural Analysis of the GGDEF-EAL Domain-Containing c-di-GMP Receptor FimX." *Structure* 17: 1104–1116.
- Navarro, M. V., P. D. Newell, P. V. Krasteva, et al. 2011. "Structural Basis for c-di-GMP-Mediated Inside-Out Signaling Controlling Periplasmic Proteolysis." *PLoS Biology* 9: e1000588.
- Newman, J. R., and C. Fuqua. 1999. "Broad-Host-Range Expression Vectors That Carry the L-Arabinose-Inducible *Escherichia coli* *araBAD* Promoter and the *araC* Regulator." *Gene* 227: 197–203.
- Nicastro, G. G., G. H. Kaihmi, T. O. Pereira, et al. 2014. "Cyclic-di-GMP Levels Affect *Pseudomonas aeruginosa* Fitness in the Presence of Imipenem." *Environmental Microbiology* 16: 1321–1333.
- Nicastro, G. G., G. H. Kaihmi, A. A. Pulschen, et al. 2020. "C-di-GMP-Related Phenotypes Are Modulated by the Interaction Between a Diguanylate Cyclase and a Polar Hub Protein." *Scientific Reports* 10: 3077.
- Nie, H., Y. Xiao, J. He, et al. 2020. "Phenotypic-Genotypic Analysis of GGDEF/EAL/HD-GYP Domain-Encoding Genes in *Pseudomonas putida*." *Environmental Microbiology Reports* 12: 38–48.
- O'Connor, J. R., N. J. Kuwada, V. Huangyutham, P. A. Wiggins, and C. S. Harwood. 2012. "Surface Sensing and Lateral Subcellular Localization of WspA, the Receptor in a Chemosensory-Like System Leading to c-di-GMP Production." *Molecular Microbiology* 86: 720–729.
- Okegbe, C., B. L. Fields, S. J. Cole, et al. 2017. "Electron-Shuttling Antibiotics Structure Bacterial Communities by Modulating Cellular Levels of c-di-GMP." *Proceedings of the National Academy of Sciences of the United States of America* 114: E5236–E5245.
- Oladosu, V. I., S. Park, and K. Sauer. 2024. "Flip the Switch: The Role of FleQ in Modulating the Transition Between the Free-Living and Sessile Mode of Growth in *Pseudomonas aeruginosa*." *Journal of Bacteriology* 206: e00365-23.
- O'Neal, L., C. Baraquet, Z. Suo, et al. 2022. "The Wsp System of *Pseudomonas aeruginosa* Links Surface Sensing and Cell Envelope Stress." *Proceedings of the National Academy of Sciences of the United States of America* 119: e2117633119.

- Orsi, E., N. J. Claassens, P. I. Nikel, and S. N. Lindner. 2021. "Growth-Coupled Selection of Synthetic Modules to Accelerate Cell Factory Development." *Nature Communications* 12: 5295.
- Orsi, E., L. Schada von Borzyskowski, S. Noack, P. I. Nikel, and S. N. Lindner. 2024. "Automated *in vivo* Enzyme Engineering Accelerates Biocatalyst Optimization." *Nature Communications* 15: 3447.
- Ozer, E. A., J. P. Allen, and A. R. Hauser. 2014. "Characterization of the Core and Accessory Genomes of *Pseudomonas aeruginosa* Using Bioinformatic Tools Spine and AGEnt." *BMC Genomics* 15: 737.
- Papenfort, K., and B. L. Bassler. 2016. "Quorum Sensing Signal-Response Systems in Gram-Negative bacteria." *Nature Reviews Microbiology* 14: 576–588.
- Poudyal, B., and K. Sauer. 2018. "The PA3177 Gene Encodes an Active Diguanylate Cyclase That Contributes to Biofilm Antimicrobial Tolerance but Not Biofilm Formation by *Pseudomonas aeruginosa*." *Antimicrobial Agents and Chemotherapy* 62: e01049-18.
- Rahme, L. G., E. J. Stevens, S. F. Wolfort, J. Shao, R. G. Tompkins, and F. M. Ausubel. 1995. "Common Virulence Factors for Bacterial Pathogenicity in Plants and Animals." *Science* 268: 1899–1902.
- Rao, F., Y. Qi, H. S. Chong, et al. 2009. "The Functional Role of a Conserved Loop in EAL Domain-Based Cyclic di-GMP-Specific Phosphodiesterase." *Journal of Bacteriology* 191: 4722–4731.
- Römling, U., M. Y. Galperin, and M. Gomelsky. 2013. "Cyclic di-GMP: The First 25 Years of a Universal Bacterial Second Messenger." *Microbiology and Molecular Biology Reviews* 77: 1–52.
- Rosenthal, V. D., H. M. Al-Abdely, A. A. El-Kholy, et al. 2016. "International Nosocomial Infection Control Consortium Report, Data Summary of 50 Countries for 2010-2015: Device-Associated Module." *American Journal of Infection Control* 44: 1495–1504.
- Ruiz, J. A., R. O. Fernández, P. I. Nikel, B. S. Méndez, and M. J. Pettinari. 2006. "dye (*Arc*) Mutants: Insights Into an Unexplained Phenotype and Its Suppression by the Synthesis of Poly(3-Hydroxybutyrate) in *Escherichia coli* Recombinants." *FEMS Microbiology Letters* 258: 55–60.
- Ryan, R. P. 2013. "Cyclic di-GMP Signalling and the Regulation of Bacterial Virulence." *Microbiology* 159: 1286–1297.
- Schäper, S., E. Krol, D. Skotnicka, et al. 2016. "Cyclic di-GMP regulates multiple cellular functions in the symbiotic alphaproteobacterium *Sinorhizobium meliloti*." *Journal of Bacteriology* 198: 521–535.
- Schindelin, J., I. Arganda-Carreras, E. Frise, et al. 2012. "Fiji: An Open-Source Platform for Biological-Image Analysis." *Nature Methods* 9: 676–682.
- Simm, R., M. Morr, A. Kader, M. Nimtz, and U. Römling. 2004. "GGDEF and EAL Domains Inversely Regulate Cyclic di-GMP Levels and Transition From Sessility to Motility." *Molecular Microbiology* 53: 1123–1134.
- Smania, A. M., I. Segura, R. J. Pezza, C. Becerra, I. Albesa, and C. E. Argaraña. 2004. "Emergence of Phenotypic Variants Upon Mismatch Repair Disruption in *Pseudomonas aeruginosa*." *Microbiology* 150: 1327–1338.
- Solano, C., B. García, C. Latasa, et al. 2009. "Genetic Reductionist Approach for Dissecting Individual Roles of GGDEF Proteins Within the c-di-GMP Signaling Network in *Salmonella*." *Proceedings of the National Academy of Sciences of the United States of America* 106: 7997–8002.
- Strempel, N., M. Nusser, A. Neidig, G. Brenner-Weiss, and J. Overhage. 2017. "The Oxidative Stress Agent Hypochlorite Stimulates c-di-GMP Synthesis and Biofilm Formation in *Pseudomonas aeruginosa*." *Frontiers in Microbiology* 8: 2311.
- Szklarczyk, D., A. L. Gable, D. Lyon, et al. 2018. "STRING v11: Protein-Protein Association Networks With Increased Coverage, Supporting Functional Discovery in Genome-Wide Experimental Datasets." *Nucleic Acids Research* 47: D607–D613.
- Timmis, K., Z. C. Karahan, J. L. Ramos, et al. 2025. "Microbes Saving Lives and Reducing Suffering." *Microbial Biotechnology* 18: e70068.
- Tischler, A. D., and A. Camilli. 2005. "Cyclic Diguanylate Regulates *Vibrio cholerae* Virulence Gene Expression." *Infection and Immunity* 73: 5873–5882.
- Toutain, C. M., M. E. Zegans, and G. A. O'Toole. 2005. "Evidence for Two Flagellar Stators and Their Role in the Motility of *Pseudomonas aeruginosa*." *Journal of Bacteriology* 187: 771–777.
- Tremblay, J., A. P. Richardson, F. Lépine, and E. Déziel. 2007. "Self-Produced Extracellular Stimuli Modulate the *Pseudomonas aeruginosa* Swarming Motility Behaviour." *Environmental Microbiology* 9: 2622–2630.
- Turlin, J., Ö. Puiggené, S. Donati, N. T. Wirth, and P. I. Nikel. 2023. "Core and Auxiliary Functions of One-Carbon Metabolism in *Pseudomonas putida* Exposed by a Systems-Level Analysis of Transcriptional and Physiological Responses." *mSystems* 8: e00004-23.
- Valentini, M., and A. Filloux. 2016. "Biofilms and Cyclic di-GMP (c-di-GMP) Signaling: Lessons From *Pseudomonas aeruginosa* and Other bacteria." *Journal of Biological Chemistry* 291: 12547–12555.
- Vasseur, P., I. Vallet-Gely, C. Soscia, S. Genin, and A. Filloux. 2005. "The *Pel* Genes of the *Pseudomonas aeruginosa* PAK Strain Are Involved at Early and Late Stages of Biofilm Formation." *Microbiology* 151: 985–997.
- Volke, D. C., L. Friis, N. T. Wirth, J. Turlin, and P. I. Nikel. 2020. "Synthetic Control of Plasmid Replication Enables Target- and Self-Curing of Vectors and Expedites Genome Engineering of *Pseudomonas putida*." *Metabolic Engineering Communications* 10: e00126.
- Volke, D. C., J. Turlin, V. Mol, and P. I. Nikel. 2020. "Physical Decoupling of XylS/*Pm* Regulatory Elements and Conditional Proteolysis Enable Precise Control of Gene Expression in *Pseudomonas putida*." *Microbial Biotechnology* 13: 222–232.
- Volke, D. C., R. A. Martino, E. Kozaeva, A. M. Smania, and P. I. Nikel. 2022. "Modular (de)construction of Complex Bacterial Phenotypes by CRISPR/Cas9-Assisted, Multiplex Cytidine Base-Editing." *Nature Communications* 13: 3026.
- Volke, D. C., K. Olavarria, and P. I. Nikel. 2021. "Cofactor Specificity of Glucose-6-Phosphate Dehydrogenase Isozymes in *Pseudomonas putida* Reveals a General Principle Underlying Glycolytic Strategies in bacteria." *mSystems* 6: e00014-21.
- Volke, D. C., N. Gurdo, R. Milanese, and P. I. Nikel. 2023. "Time-Resolved, Deuterium-Based Fluxomics Uncovers the Hierarchy and Dynamics of Sugar Processing by *Pseudomonas putida*." *Metabolic Engineering* 79: 159–172.
- Volke, D. C., E. Orsi, and P. I. Nikel. 2023. "Emergent CRISPR-Cas-Based Technologies for Engineering Non-model bacteria." *Current Opinion in Microbiology* 75: 102353.
- Wang, F., Q. He, J. Yin, S. Xu, W. Hu, and L. Gu. 2018. "BrlR From *Pseudomonas aeruginosa* Is a Receptor for Both Cyclic di-GMP and Pyocyanin." *Nature Communications* 9: 2563.
- Waters, C. M. 2018. "Shining the Light on Cyclic di-GMP Dark Matter." *Journal of Bacteriology* 200: e00030-18.
- Winsor, G. L., E. J. Griffiths, R. Lo, B. K. Dhillon, J. A. Shay, and F. S. Brinkman. 2016. "Enhanced Annotations and Features for Comparing Thousands of *Pseudomonas* Genomes in the *Pseudomonas* Genome Database." *Nucleic Acids Research* 44: D646–D653.
- Winstanley, C., S. O'Brien, and M. A. Brockhurst. 2016. "*Pseudomonas aeruginosa* Evolutionary Adaptation and Diversification in Cystic Fibrosis Chronic Lung Infections." *Trends in Microbiology* 24: 327–337.
- Wirth, N. T., N. Gurdo, N. Krink, et al. 2022. "A Synthetic C2 Auxotroph of *Pseudomonas putida* for Evolutionary Engineering of Alternative Sugar Catabolic Routes." *Metabolic Engineering* 74: 83–97.

Wirth, N. T., E. Kozaeva, and P. I. Nickel. 2020. “Accelerated Genome Engineering of *Pseudomonas putida* by I-SceI—Mediated Recombination and CRISPR-Cas9 Counterselection.” *Microbial Biotechnology* 13: 233–249.

Wirth, N. T., J. Funk, S. Donati, and P. I. Nickel. 2023. “*QurvE*: User-Friendly Software for the Analysis of Biological Growth and Fluorescence Data.” *Nature Protocols* 18: 2401–2403.

Wirth, N. T., K. Rohr, A. Danchin, and P. I. Nickel. 2023. “Recursive Genome Engineering Decodes the Evolutionary Origin of an Essential Thymidylate Kinase Activity in *Pseudomonas putida* KT2440.” *mBio* 14: e01081-23.

Wu, X., S. Monchy, S. Taghavi, W. Zhu, J. L. Ramos, and D. van der Lelie. 2011. “Comparative Genomics and Functional Analysis of Niche-Specific Adaptation in *Pseudomonas putida*.” *FEMS Microbiology Reviews* 35: 299–323.

Xiao, R., L. Chun, E. A. Ronan, D. I. Friedman, J. Liu, and X. Z. Xu. 2015. “RNAi Interrogation of Dietary Modulation of Development, Metabolism, Behavior, and Aging in *C. elegans*.” *Cell Reports* 11: 1123–1133.

Supporting Information

Additional supporting information can be found online in the Supporting Information section.